


For Reference

NOT TO BE TAKEN FROM THIS ROOM

Ex LIBRIS
UNIVERSITATIS
ALBERTAENSIS





Digitized by the Internet Archive
in 2023 with funding from
University of Alberta Library

<https://archive.org/details/Lemieux1977>

THE UNIVERSITY OF ALBERTA

A NUCLEAR MAGNETIC RESONANCE STUDY OF GADOLINIUM (III) ION
BINDING TO ADENOSINE TRIPHOSPHATE AND INOSINE TRIPHOSPHATE

BY



ANDRE LEMIEUX

A THESIS

SUBMITTED TO THE FACULTY OF GRADUATE STUDIES AND RESEARCH
IN PARTIAL FULFILMENT OF THE REQUIREMENTS FOR THE DEGREE

OF

MASTER OF SCIENCE

DEPARTMENT OF CHEMISTRY

EDMONTON, ALBERTA

SPRING, 1977

TO MY FAMILY

ABSTRACT

A nuclear magnetic resonance (NMR) study was carried out on adenosine 5'-triphosphate (ATP) and inosine 5'-triphosphate in the presence of the paramagnetic metal ion gadolinium (III). Phosphorus-31 transverse (T_{2p}) and longitudinal (T_{1p}) relaxation times due to the paramagnetic metal ion were obtained for both nucleotides as a function of temperature. These data were then compared with those for a transition metal ion - nucleotide system (Mn(II)-ATP) where an interaction with both the adenine ring and the triphosphate chain has been observed. ^{13}C data show that for the gadolinium (III) ATP and ITP complexes there is no ring interaction. The temperature dependence of T_{1p} and T_{2p} for the ^{31}P nuclei also differs in form from that observed for the manganese (II) system.

A kinetic study was carried out on the Gd(III)-ITP system. The data can best be analysed by postulating a $\text{Gd}(\text{ITP})_2$ species in solution, since a simple 1:1 Gd(ITP) complex cannot explain the observed effects.

ACKNOWLEDGEMENTS

I would like to express my grateful thanks to all of the following:

Dr. G. Kotowycz for his guidance and help during the course of this research.

Drs. G.P.P. Kuntz and Y.F. Lam for their invaluable discussions and suggestions.

Dr. R.B. Jordan for his assistance in obtaining the multiple frequency spectra.

Dr. D. Rabenstein for his suggestions after proofreading the initial manuscript.

Mrs. Sandra O'Shaughnessy for the typing of the manuscript.

TABLE OF CONTENTS

CHAPTER		PAGE
ONE	INTRODUCTION.....	1
TWO	THEORY.....	5
	Transverse Relaxation.....	5
	Longitudinal Relaxation.....	11
THREE	EXPERIMENTAL.....	17
	Preparation of Solutions.....	17
	NMR Experiments.....	18
	(a) Phosphorus T_2 Measurements.....	18
	(b) Phosphorus T_1 Measurements.....	19
	(c) Carbon T_2 Measurements.....	20
	(d) Phosphorus Multiple Frequency T_1 Measurements.....	20
FOUR	RESULTS	22
FIVE	DISCUSSION.....	42
	Kinetic Study of Gd(III)-ITP.....	46
	CASE 1: No ML_2 in solution.....	48
	CASE 2: ML_2 in Solution.....	50
	BIBLIOGRAPHY.....	54

LIST OF TABLES

<u>TABLE</u>		<u>PAGE</u>
I	T_2 Measurements for the α and γ phosphorus of Gd(III)-ATP solutions.....	28
II	T_1 Measurements for the α , β and γ phosphorus of Gd(III)-ATP solutions.....	30
III	T_2 Measurements for the α and γ phosphorus of Gd(III)-ITP solutions.....	32
IV	T_1 Measurements for the α , β and γ phosphorus of Gd(III)-ITP solutions.....	34
V	^{31}P Average values of T_2 and T_1 , obtained for Gd(III)-ATP.....	36
VI	^{31}P Average values of T_2 and T_1 , obtained for Gd(III)-ITP.....	38

LIST OF FIGURES

<u>FIGURE</u>		<u>PAGE</u>
1	Adenosine 5'-triphosphate (ATP) and Inosine 5'-triphosphate.....	2
2	^{13}C NMR spectra of ATP as a function of Gd(III) concentration.....	25
3	^{13}C NMR spectra of ITP as a function of Gd(III) concentration.....	27
4	Plot of $(f_m T_{2p})^{-1}$ vs T^{-1} for Gd(III)-ATP.....	29
5	Plot of $(f_m T_{1p})^{-1}$ vs T^{-1} for Gd(III)-ATP.....	31
6	Plot of $(f_m T_{2p})^{-1}$ vs T^{-1} for Gd(III)-ITP.....	33
7	Plot of $(f_m T_{1p})^{-1}$ vs T^{-1} for Gd(III)-ITP.....	35
8	Plot of $(f_m T_{2p})^{-1}$ and $(f_m T_{1p})^{-1}$ vs T^{-1} for Gd(III)-ATP.....	37
9	Plot of $(f_m T_{2p})^{-1}$ and $(f_m T_{1p})^{-1}$ vs T^{-1} for Gd(III)-ITP.....	39
10	Plot of $\Delta\nu$ vs T^{-1} for Gd(III)-ITP where [ITP] varies by a factor of ten.....	41

11	Plot of $(f_{m2p} T)^{-1}$ vs T^{-1} for Gd(III)-ITP where [ITP] varies by a factor of ten.....	49
----	--	----

CHAPTER ONE

INTRODUCTION

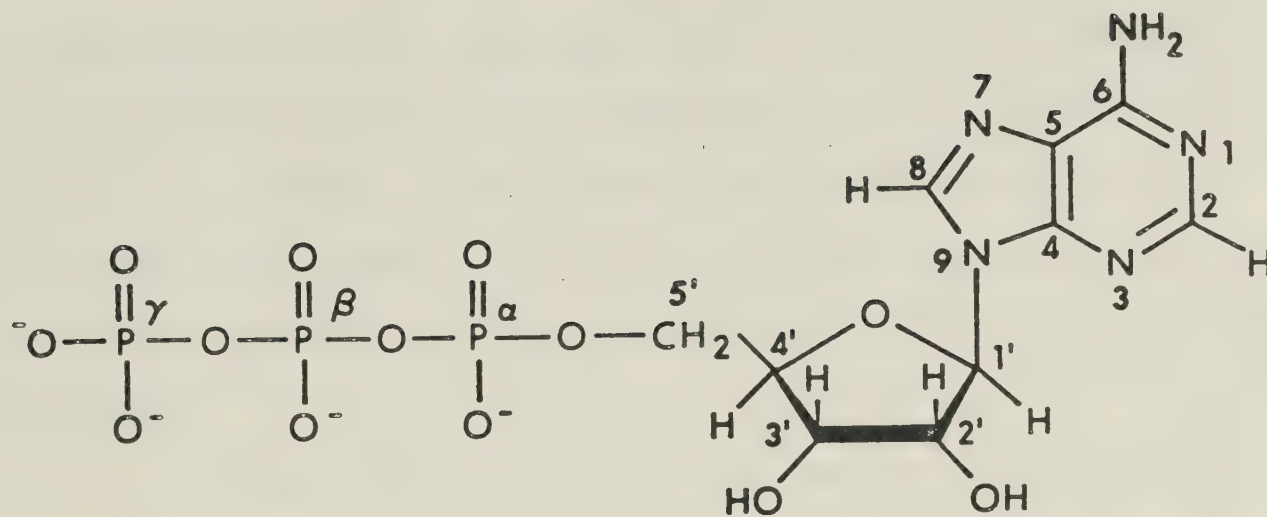
The enzymatic hydrolysis of the nucleotide phosphate chain is probably one of the most important energy transfer reactions in biological systems (1) and certain metal ions take part as essential substrates in these reactions. As a result, very many studies concerning the role of metal ions in biological systems have been carried out and have now been well reviewed by Izatt et al, (2) Dwek (3) and Sigel (4).

The metal ion - nucleotide interactions are of great interest. Of particular interest is the metal ion manganese (II) whose paramagnetic behavior allows for the study of biological systems through the use of nuclear magnetic resonance techniques. It should be noted here that, although Mn(II) is not an active metal ion in vivo, it has been found to substitute quite well in vitro for Mg(II) in many enzymatic reactions (5,6).

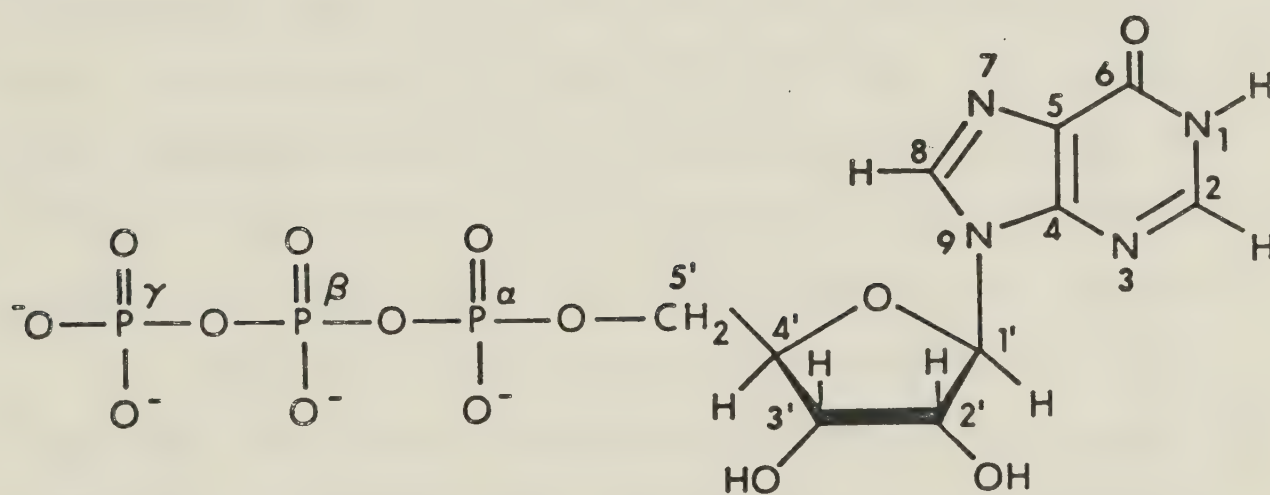
Of all naturally occurring nucleotides, adenosine triphosphate (ATP) (Figure 1) is the most common and its interaction with Mn(II) ions has been the subject of much attention (7-15). These studies indicate that the metal ion is completely bound by all three phosphate groups although the distance to the "α" phosphorus is longer than to the "β" and "γ" phosphorus nuclei (11). In addition, 20% of the bound Mn(II) ions coordinate directly with the adenine ring at the N-7 position (9)

The interaction of lanthanide ions with biological systems has also been the subject of much research. The general purpose of the

FIGURE 1



Adenosine 5' - Triphosphate ATP



Inosine 5' - Triphosphate ITP

work has been directed towards studying the feasibility of using lanthanide ions as paramagnetic models for the alkaline earth ions (7, 16-20) and certain transition metals (21,22). It has been observed, for instance, that in the case of enzymes (17,20) and various nucleotides (2,23-28), lanthanide ions bind only to the phosphate groups (unlike Mn(II)), and that this effect is of an electrostatic nature. In addition, it also appears that the interaction is the same with all phosphates as in the case of alkali metals (29) where there is some question of higher order species (29,30) (i.e. M_2L , M_2L_2 etc.).

A very recent study on the conformation of the lanthanide ion - ATP complexes in solution has been carried out (Ln(III)=Pr, Nd, Eu, and Yb) (23). Chemical shift data of the eight proton resonances and of the three ^{31}P resonances were obtained. The analysis of the data indicates that the lanthanide ions bind predominately to the β and γ phosphates and do not interact with the ring. The distance to the α phosphate is nearly twice as large as to the β and γ phosphates. For the Gd(III)-ATP complex, T_{1p} measurements were also carried out for protons H-8, H-2, H-1' and H-5' but ^{31}P studies were not reported.

The object of the present work is to compare the Gd(III) - nucleotide complexes with the corresponding Mn(II) ion complexes that have been extensively studied. The nucleoside triphosphates under study are adenosine 5' - triphosphate and inosine 5' - triphosphate (Figure 1). The experimental techniques used are ^{13}C and ^{31}P NMR. With a total of thirteen different nuclear probes that can be observed readily, the effects of the paramagnetic Gd(III) ion on the relaxation time of

these nuclei can be easily studied. The results shed further light on the nature of these complexes in solution as well as the exchange processes taking place.

CHAPTER TWO

THEORY

The paramagnetic lanthanide metal ion (gadolinium (III)) is used primarily as a broadening reagent in NMR studies. In fact, the paramagnetic broadening effects are so large that the NMR experiments are usually carried out under conditions where the metal ion concentration is much less than the ligand concentration. Paramagnetic relaxation data is then extracted from a resonance signal which is a weighted average of the metal-bound and metal-free nucleotide system undergoing exchange in solution.

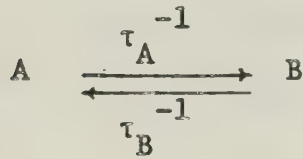
In the present chapter, the theory concerning both the transverse (T_{2p}) and longitudinal (T_{1p}) relaxation times due to the paramagnetic metal ion will be introduced and analyzed with respect to the paramagnetic lanthanide ion Gd(III). Since these relaxation times are proportional to r^{-6} , where r is the distance from the paramagnetic ion to the nucleus under observation, these studies offer a way of obtaining structural information about the metal ion - nucleotide complexes. In addition, these data yield information concerning the exchange rate in solution.

Transverse Relaxation

McConnell's (31) addition of "chemical exchange" to the Bloch (32) equations was later followed by the Swift and Connick (33) refinement for a two-site exchange. Swift and Connick considered the case where the concentration of one of the components is in

large excess.

Consider a two - site exchange process:



where τ_A^{-1} and τ_B^{-1} are pseudo - first order rate constants relating to the exchange rate from sites A or B. Then, for the case $P_A \gg P_B$ (where P_i is the fraction in the i^{th} state), one obtains (34)

$$v \approx v_A = \frac{\omega_1 M_0 (T_{2A}^{-1} + T_{2P}^{-1})}{(T_{2A}^{-1} + T_{2P}^{-1})^2 + (\Delta\omega_A + \Delta\omega_P)^2} \quad [1]$$

where

$$T_{2P}^{-1} = \frac{1}{\tau_A} \left[\frac{T_{2B}^{-2} + (T_{2B}\tau_B)^{-1} + (\omega_{0B} - \omega)^2}{(T_{2B}^{-1} + \tau_B^{-1})^2 + (\omega_{0B} - \omega)^2} \right] + T_{2os}^{-1} \quad [2]$$

$$\Delta\omega_P = \frac{(\omega_{0B} - \omega) / \tau_A \tau_B}{(T_{2B}^{-1} + \tau_B^{-1})^2 + (\omega_{0B} - \omega)^2} \quad [3]$$

$$\Delta\omega_A = \omega_{0A} + \omega \quad [4]$$

The terms in these equations are defined as follows:

T_2 = Transverse relaxation time.

M_0 = Magnetization vector in the direction of the applied field.

ω_0 = Angular precession frequency about the applied field

ω_1 = Angular precession frequency about the applied r.f. field H_1

ω = Observed angular frequency which is a weighted average of ω_A and ω_B .

T_{2os} = Outer sphere transverse relaxation time.

ν = Observed resonance frequency.

The above equations apply to "Paramagnetic - Diamagnetic" exchange, where site A is considered to be the free ligand and site B is the metal ion - ligand complex. Under these conditions one finds that the term $(\omega_{OB} - \omega_{OA})$ may become quite large (i.e. $\sim 10^6 \text{ sec}^{-1}$), due to the effect of the unpaired electrons on the metal ion. Since $\omega \approx \omega_{OA}$ it can be seen that the term $(\omega_{OB} - \omega)$ is usually also large.

The limiting cases of equation 2 have been discussed in detail (33,34,35) and it is found that the increase in the transverse relaxation rate induced by the paramagnetic ion (T_{2p}^{-1}) can be analyzed in terms of three limiting cases.

CASE I: Slow Exchange $\Delta\omega_B^2 \gg T_{2B}^{-2}, \tau_B^{-2}$

The relaxation rate is governed by the rate of chemical exchange of molecules between the bulk solvent (A) and the bound complex (B), including outer sphere effects. Therefore equation 2 becomes

$$T_{2p}^{-1} = \tau_A^{-1} + T_{2os}^{-1} = (P_B/P_A)\tau_B^{-1} + T_{2os}^{-1} \quad [5]$$

CASE II: Exchange Narrowing $\tau_B^{-2} \gg \Delta\omega_B^2 \gg (T_{2B} \tau_B)^{-1}$

In this case the relaxation rate is controlled by the change in the precessional frequency plus outer sphere effects.

$$\text{Therefore } T_{2p}^{-1} = (P_B/P_A) \tau_B \Delta\omega_B^2 + T_{2os}^{-1} \quad [6]$$

CASE III: Fast Exchange $(T_{2B} \tau_B)^{-1} \gg T_{2B}^{-2}, \Delta\omega_B^{-2}$

The observed relaxation rate is now controlled by the relaxation rate of the nucleus when it is bound to the metal ion together with outer sphere relaxation.

$$\text{Therefore } T_{2p}^{-1} = (P_B/P_A) T_{2B}^{-1} + T_{2os}^{-1} \quad [7]$$

Many paramagnetic systems are referred to as "broadening" rather than "shift" reagents. One usually notes that for the former case significant broadening of the observed resonance occurs with little or no chemical shift. This phenomenon is believed to be due to highly efficient relaxation of the bound sphere nuclei such

that $T_{2B}^{-2} \gg \Delta\omega_B^2$. As a result, a temperature dependence study of transverse relaxation rates will not show an "exchange narrowing" limit (i.e. no region where T_{2p}^{-1} depends on $\Delta\omega_B$) (34).

Hence equation 2 reduces to:

$$T_{2p}^{-1} = \frac{(P_B/P_A)}{T_{2B} + \tau_B} + T_{2os}^{-1} \quad [8]$$

From now on, the bound state "B" will be referred to as "M" and equation 8 can now be rewritten in the more common form:

$$T_{2p}^{-1} = \frac{f_m}{T_{2M} + \tau_M} + T_{2os}^{-1} \quad [9]$$

$$\text{where } f_m = P_M/P_A$$

$$\text{and } \tau_M = \tau_B$$

The various terms in equation 9 will now be discussed in detail:

$$\underline{\underline{\tau_M^{-1}}}$$

This term is a measure of the rate of chemical exchange of molecules between the bulk solvent and the metal ion complex. It is often described as a "pseudo" first order rate constant "k". The temperature dependence of τ_M is given by:

$$k_1 = \tau_M^{-1} = \frac{kT}{h} \exp \left(\frac{-\Delta H^\ddagger}{RT} + \frac{\Delta S^\ddagger}{R} \right) \quad [10]$$

where k is the Boltzmann constant, h is Planck's constant, T is the temperature in degrees Kelvin, R is the ideal gas constant and ΔH^\ddagger and ΔS^\ddagger are the enthalpy and entropy of activation, respectively.

$$\underline{\underline{T_{2M}^{-1}}}$$

Solomon and Bloembergen (36,37) have derived an expression for the relaxation of the nucleus bound to the metal ion (T_{2M}^{-1}) where it is assumed that the Larmor precession frequency of the electrons ω_S is greater than that for the nucleus ω_I (i.e. $\omega_S \gg \omega_I$). In addition, Connick and Fiat (38) have modified the equation to incorporate the two different dipolar correlation times τ_{C1} and τ_{C2} . The equation may be written as

$$T_{2M}^{-1} = \frac{\gamma_I^2 g^2 S(S+1) \beta^2}{15r^6} \left[4\tau_{c1} + \frac{3\tau_{c1}}{1 + \omega_I^2 \tau_{c1}^2} + \frac{13\tau_{c2}}{1 + \omega_S^2 \tau_{c2}^2} \right] \quad [11]$$

$$+ \frac{1}{3} S(S+1) (A/\hbar)^2 \left[\tau_{e1} + \frac{\tau_{e2}}{1 + \omega_S^2 \tau_{e2}^2} \right]$$

where:

$$\tau_{C1}^{-1} = \tau_R^{-1} + \tau_{e1}^{-1} = \tau_R^{-1} + \tau_M^{-1} + T_{1e}^{-1} \quad [12]$$

$$\tau_{C2}^{-1} = \tau_R^{-1} + \tau_{e2}^{-1} = \tau_R^{-1} + \tau_M^{-1} + T_{2e}^{-1} \quad [13]$$

In equations 12 and 13, τ_R is the rotational tumbling time of the metal-ligand complex, τ_M is the average lifetime of the ligand-metal coupled pair (see equation 10), T_{1e} is the longitudinal and T_{2e} is the transverse electronic relaxation time, respectively.

The terms in equation 11 are defined as follows:

γ_I = Magnetogyric ratio

β = Bohr magneton

- g = Electron g factor
 S = Total electron spin of the metal ion
 ω_S = Electron resonance frequency
 ω_I = Nuclear resonance frequency
 r = Distance between the nucleus and the paramagnetic ion
 (A/\hbar) = Electron nuclear hyperfine coupling constant.

$$\underline{\underline{T_{2os}^{-1}}}$$

Contributions to the line broadening resulting from outer sphere effects are the result of magnetic dipole - dipole interactions between the metal ion and molecules outside the metal ion first co-ordination sphere. A general formulation for this effect has been developed (39) and is given by the following equation:

$$T_{2os}^{-1} = \frac{16\pi}{9} \frac{nS(S+1)\beta^2 g^2 \gamma_I^2 \tau_c}{r^3} \quad [14]$$

where n is the number of paramagnetic ions per cubic centimeter of solution and τ_c is the dipolar correlation time comprising exchange, tumbling and electronic effects.

Longitudinal Relaxation

Luz and Meiboom (39) have developed an expression for T_{1p}^{-1} similar to that obtained for T_{2p}^{-1} by Swift and Connick (33). The equation may be written as follows:

$$T_{1p}^{-1} = \frac{f_m}{T_{1M} + \tau_M} + T_{1os}^{-1} \quad [15]$$

In the above equation, both the outer sphere (T_{1os}^{-1}) term

and the chemical exchange (τ_M) lifetime are the same as those for equation 9 (i.e. $T_{1cs} = T_{2os}$). The (T_{1M}^{-1}) term, however, is different from T_{2M}^{-1} and is also described by Solomon and Bloembergen (36,37), Connick and Fiat (38) and Rubinstein et al (40). It is given by the following equation:

$$T_{1M}^{-1} = \frac{2\gamma_I^2 g^2 S(S+1)\beta^2}{15r^6} \left[\frac{3\tau_{c1}}{1 + \omega_I^2 \tau_{c1}^2} + \frac{7\tau_{c2}}{1 + \omega_S^2 \tau_{c2}^2} \right] + \frac{2}{3} (A/\hbar)^2 S(S+1) \left[\frac{\tau_{e2}}{1 + \omega_S^2 \tau_{e2}^2} \right] \quad [16]$$

The terms in this equation have been defined previously for equation 11.

Factors Affecting T_{1M} and T_{2M} :

The expressions for T_{1M}^{-1} and T_{2M}^{-1} given by Solomon and Bloembergen do contain certain restrictions which should be discussed. The first states that there is no electronic (i.e. g) anisotropy, a condition which is satisfied by both Mn(II) and Gd(III) (3), and secondly that there is only one value for T_{1e} and one for T_{2e} , respectively.

Rubinstein (40) and co workers have calculated exact values for the electronic relaxation times for a system where $S = 5/2$ (Mn(II)). They obtained three different spin-spin and spin-lattice electronic relaxation times, each of which had a corresponding intensity factor whose magnitude depended on the value of the $\omega_S \tau_V$ term. This latter

term originates from the Bloembergen and Morgan (41) equation which presents a general formulation for calculating the longitudinal electron relaxation time (T_{1e}), namely:

$$T_{1e}^{-1} = B \left[\frac{\tau_v}{1 + \omega_s^2 \tau_v^2} + \frac{4\tau_v}{1 + 4\omega_s^2 \tau_v^2} \right] \quad [17]$$

In this equation, τ_v is a correlation time which relates to the rate at which the Zero Field Splitting (ZFS) is modulated by the impact of the solvent molecules. The restrictions imposed on this expression are that $\tau_v < T_{1e}$, $T_{2e} \ll T_{1e}$ and also that the magnitude of the ZFS be less than ω_s . Rubinstein et al (40) observed that four of the intensity factors for the electronic relaxation times approached zero when $\omega_s^2 \tau_v^2 \ll 1$. Hence under these conditions only one T_{1e} and one T_{2e} value are observed and therefore satisfy the previously mentioned restriction for the Solomon-Bloembergen equations.

It is important to note here that the activation energy (E_v) for the motion characterized by τ_v is given by:

$$\tau_v = \tau_o \exp (E_v/RT) \quad [18]$$

Therefore, as T increases, τ_v decreases and hence T_{1e}^{-1} will show a positive change providing $\omega_s^2 \tau_v^2 \ll 1$.

Hudson and Lewis (42) treated a system where $S = 7/2$ (Gd(III)) in a manner similar to that of Rubinstein et al (40) and obtained four values of T_{2e} each of which had a corresponding intensity factor. As for Mn(II), it was observed that when $\omega_s \tau_v < 1$, only one of the four spin - spin relaxation times was found to dominate. Unlike Mn(II), however, for which the EPR spectrum consists of six lines due to nuclear hyperfine effects (40), Gd(III) showed only a single

line rather than the expected seven since the $-1/2 \rightarrow +1/2$ transition contributes most (i.e. 96%) to the observable signal (42). The fact that T_{2e} may be obtained directly from the spectrum has led Dwek (35) to speculate that the value of the "B" and " τ_v " terms in equation 17 may then be calculated to obtain a value for T_{1e} .

Reuben (21) has obtained values for the correlation time modulating electron spin relaxation for three different systems containing gadolinium (III). These values were then compared to similar systems containing manganese (II) and it was observed that the size of the ligand did not, for either metal ion, significantly change the value of τ_v (i.e. 5×10^{-12} sec at 300° K). In addition, it was also noted that for experiments carried out at a magnetic field of 12.1 kilogauss, a value of $\omega_s = 2 \times 10^{11}$ sec $^{-1}$ and a range of T_{2e}^{-1} in the vicinity of $1 \times 10^9 \sim 3 \times 10^9$ sec were obtained depending on the value of τ_v (i.e. size of ligand). Hence it may be concluded that for Gd (III), like in the case of Mn(II) (40), $(\omega_s \tau_{c2})^2 > 1$, for a magnetic field strength of 12.1 kilogauss or greater; since as the field strength increases, ω_s increases and T_{2e}^{-1} decreases.

Applying this limit, equations 11 and 16 can be rewritten as:

$$T_{2M}^{-1} = \frac{\gamma_I^2 g^2 S(S+1) \beta^2}{15r^6} \left[4\tau_{c1} \frac{3\tau_{c1}}{1+\omega_I^2 \tau_{c1}^2} \right] + \frac{1}{3} S(S+1) (A/\pi)^2 \tau_{e1} \quad [19]$$

$$T_{1M}^{-1} = \frac{2\gamma_I^2 g^2 S(S+1) \beta^2}{15r^6} (3\tau_{c1} / 1 + \omega_I^2 \tau_{c1}^2) \quad [20]$$

At this point, it would be of interest to consider the various terms in equations 11 and 16 to see how they affect the observed relaxation times T_{1p} and T_{2p} . Each of these equations are made up of two terms, a dipolar term (first portion of equation) and a scalar term (remaining portion). The scalar term is usually absent from relaxation expressions for lanthanide ions due presumably to the small $(A/h)^2$ term (35). This argument is further supported by noting that contact or scalar terms are due to the "leakage" of unpaired electrons from the metal to the ligand. Such effects are not expected to occur too readily in lanthanides where the valence (4f) electrons are in effect buried (35). If only the dipolar portions of equations 19 and 20 are considered, then it can be seen that T_{2M}^{-1} and T_{1M}^{-1} are nearly equal (i.e. within 14%) providing that $(\omega_I \tau_{cl})^2 < 1$.

Returning back to the expression for T_{1p} (eq. 15), it can be seen that a negative value for $d(1/T_{1p}) / d(1/T)$ can arise from three possible sources (3,11):

- (1) T_{1p}^{-1} is controlled by the slow exchange mechanism (τ_M^{-1}) .
- (2) T_{1p}^{-1} is controlled by the fast exchange mechanism where $(\omega_I \tau_{cl})^2 < 1$ and T_{1e} is the dominant correlation time exhibiting a negative activation energy.
- (3) T_{1p}^{-1} is controlled by the fast exchange mechanism when $(\omega_I \tau_{cl})^2 > 1$ and the dominant correlation time, which may be either τ_M , τ_R or T_{1e} , has a positive activation energy.

When a negative slope is observed, which is controlled by T_{1M}^{-1} (i.e. case (2) or (3)), then T_{1p}^{-1} is expected to show a frequency dependence. If $(\omega_I \tau_{cl})^2 > 1$, then this term becomes a significant factor in equation 20, and therefore a change in frequency (i.e. ω_I) will cause a notable change in the value of T_{1p}^{-1} (equation 15). If, on the other hand, $(\omega_I \tau_{cl})^2 < 1$ then, as indicated in case (2), T_{1e} becomes the dominant term in the expression for τ_{cl} . The activation term (E_v) that is involved here is given by equation 18 and the negative value for the activation energy originates from the term $(\omega_s \tau_v)^2$ in equation 17. In other words, since $T_{1p}^{-1} \propto T_{1M}^{-1} \propto \tau_{cl}^{-1} \propto T_{1e}^{-1}$ (equations 12, 15 and 20) in case (2), and since $\tau_v \propto 1/T$ (equation 18), a negative activation energy is possible for T_{1e}^{-1} only if $T_{1e}^{-1} \propto \tau_v^{-1}$ (equation 17). This conclusion implies that $(\omega_s \tau_v)^2 > 1$ and under such a condition a change in frequency (ω_s) will also change T_{1p}^{-1} (equation 17).

In this section, expressions have been given for both τ_M and T_{1e} . For completeness, the temperature dependence of the rotational correlation time should also now be included. It is given by the following equation:

$$\tau_R = \tau_R^0 \exp (E_r/RT) \quad [21]$$

It is interesting to note the similarity between equation 21 and both equations 18 and 10. The fact that all three correlation times relating to the three different types of mechanisms show an exponential energy dependence is another of the restrictions for the Solomon-Bloembergen equations (3).

CHAPTER THREE

EXPERIMENTAL

Preparation of Solutions

ATP (disodium salt) and ITP (sodium salt) of highest purity grade were obtained from Sigma Chemical Company. Each nucleotide salt was then dissolved in triply distilled water, passed through a CHELEX 100 (sodium form) exchange resin to remove metal ion impurities, and then the pH was set at 7.0 ± 0.2 . Solutions were then lyophilized at least twice from D_2O , obtained from Columbia Organic Chemical Company, and the nucleotide concentrations were determined by U. V. Spectroscopy. (ATP, $\epsilon_{\max} = 1.57 \times 10^4$, 260 nm, pH = 7.0; ITP, $\epsilon_{\max} = 1.22 \times 10^4$, 270 nm, pH = 6.6). These concentrations were between 0.3M and 0.6M for both nucleotides, and the final solutions were made up to a volume of 2 mls in D_2O .

Stock solutions of Gd(III) were prepared from $Gd(NO_3)_3 \cdot 5H_2O$ obtained from Ventron Alfa Products. The solutions were made up to 0.1M and acidified to a pH = 1. H. E. Pedersen micropipets were used to make metal ion additions.

Standardization (43) of two Gd(III) stock solutions was carried out by adding Eriochrome Black T indicator to a solution of 25 mls $Gd(NO_3)_3$; 75 mls of H_2O ; 10 mls of NH_4Cl buffer (pH = 9.9) and a small amount of triethanolamine (1 - 2 mls). The red solution was then titrated with E.D.T.A. until the blue color of free indicator appeared. The results obtained from this procedure were in good

agreement ($\pm 4\%$) with the concentrations calculated from the weight of the nitrate salt used for each stock solution. As a result, no further standardizations were deemed necessary and the concentrations of new stock solutions were assumed to equal those calculated from the amount of salt used.

A 0.9M solution of tetramethyl ammonium nitrate (obtained from Eastman Kodak Company) was prepared in D_2O and used in the kinetic study (see table VIII) to adjust the ionic strength of the 0.01M ITP solution to that for the 0.1M ITP solution (I.E. $\mu = 1.0M$).

NMR Experiments

(a) Phosphorus Paramagnetic Transverse Relaxation Time Measurements

$$\underline{(T_{2p})}$$

Transverse relaxation times were measured from the linewidths at half height of the natural abundance, proton decoupled ^{31}P NMR spectra obtained in the Fourier transform mode on a Bruker HFX 90 NMR spectrometer (36.43 MHz). All measurements were carried out under controlled temperature conditions ($\pm 1^\circ$). The D_2O solvent deuterium resonance was used as the lock signal. The resulting FID signals were stored in a Nicolet computer and the Fourier transformed spectra (real) were recorded using 4K or 2K data points depending on the required resolution for a sweep width of 3000 Hz.

The effective paramagnetic linewidth " $\Delta\nu_{\frac{1p}{2}}$ " was calculated by subtracting the observed linewidth at half height of a pure nucleotide resonance " $\Delta\nu_{\frac{1A}{2}}$ " from that of a comparable nucleotide resonance in the presence of the metal ion " $\Delta\nu_{\frac{1M}{2}}$ ",

$$\Delta\nu_{1/2,P} = \Delta\nu_{1/2,M} - \Delta\nu_{1/2,A} = 1/\pi T_{2p} \quad [22]$$

For spectra where sufficient resolution of the α and γ phosphorus "doublets" could not be observed; corrections were made for a $J(31p - 31p)$ splitting of 19.5 Hz while calculations for the β phosphorus triplet were omitted.

(b) Phosphorus Paramagnetic Longitudinal Relaxation Time Measurements

(T_{1p})

Spin-lattice relaxation times were evaluated from proton decoupled, partially relaxed, Fourier transformed spectra obtained using the $(-180^\circ - \tau - 90^\circ - T -)_n$ (44,45) two pulse sequence. The natural abundance ^{31}P NMR spectra were obtained on a Varian HA - 100 - 15 NMR spectrometer (40.48 MHz) interfaced with a Digilab FTS/NMR-3 data system, the Nova 1200 computer, and the FTS/NMR 400-2 pulse unit. Probe temperatures were measured directly with a thermometer ($\pm 1^\circ C$), and again the deuterium resonance of the solvent D_2O was used as the lock signal. All required resonances were found to be within 2700 Hz of the carrier frequency and were recorded using 2K data points. All longitudinal relaxation times were obtained from at least seven different τ values.

For any given value of τ , a value for the average peak height (H_T) was obtained for both the α and γ doublets. Each of these values, along with the one obtained for the β triplet (i.e. peak height of the central peak for the β triplet), were subtracted from the corresponding maximum peak heights (H_{max}) obtained when $\tau = \infty$ (i.e. $\tau \geq 5 T_1$). The logarithm of the resulting parameter

$H(H = H_{\max} - H_{\tau})$ was then plotted against the corresponding " τ " value and the longitudinal relaxation times were calculated from the graphs using the following equation (19)

$$\ln H = \ln(2H_{\max}) - \frac{\tau}{T_1} \quad [23]$$

The longitudinal relaxation time due to the presence of paramagnetic metal ions was obtained by subtracting the T_{1A}^{-1} value obtained for the purified nucleotide from the T_{1Me}^{-1} value obtained for the corresponding resonance in the presence of the paramagnetic ion, namely:

$$T_{1p}^{-1} = T_{1Me}^{-1} - T_{1A}^{-1} \quad [24]$$

(c) Carbon-13 Paramagnetic Transverse Relaxation Time Measurements

(T_{2p})

Instrumental conditions for obtaining the carbon-13 NMR spectra were exactly the same as those for phosphorus except that the spectrometer frequency was set at 22.63 MHz (Bruker HFX-90). In addition, the FID signals were stored in 16K or 8K data points and consequently the Fourier transformed spectra were outputted using 8K or 4K data points, respectively.

(d) Phosphorus Multiple Frequency Longitudinal Relaxation Time Measurements (T_{1p})

A Bruker SXP 4-100 NMR spectrometer (using a two pulse $-180^\circ - \tau - 90^\circ$ sequence) was used to obtain ^{31}P spectra for the α , β and γ phosphates of (Gd - ITP) at two different frequencies. Each spectrum was the result of a single scan performed at variable τ values under ambient temperature conditions. A diode output of

the combined FID for the α , β and γ phosphorus nuclei was obtained at a frequency of 23.98 MHz. The appearance of a null point at 50 ms delay time validated the original assumption that the longitudinal relaxation times of all three phosphorus nuclei were equal. At 12.20 MHz a higher sensitivity non-rectified output of the FID also yielded a null point in the 50 ms range. The nucleotide concentration was [ITP] = 0.25 M and the metal ion concentration was [Gd(III)] = 3.7×10^{-4} M.

I am very grateful to Dr. R. B. Jordan for conducting this experiment.

CHAPTER FOUR

RESULTS

The ^{13}C NMR spectrum of ATP is shown in Figure 2. The ^{13}C lines were assigned in accordance with previous work (46,47,48). Progressive addition of metal ions to both ATP and ITP solutions caused a selective broadening of the C-5', C-4' and C-3' resonances for both nucleotides. A weaker broadening effect was observed for the ATP C-8 resonance, in contrast to ITP (Figure 3) where this effect was not observed.

Figures 4 to 9 inclusive are graphs of the ^{31}P , T_{2p}^{-1} and T_{1p}^{-1} data as a function of the temperature for both ATP and ITP. The T_{1p}^{-1} data in Figures 5 and 7 were obtained for all three (α , β and γ) phosphorus nuclei, whereas the T_{2p}^{-1} data in Figures 4 and 6 were obtained for the α and γ phosphorus nuclei only. It should be noted that at lower temperatures (i.e. sharper lines), we found that the T_{2p}^{-1} for the β phosphorus was equal, within experimental error, to the transverse relaxation times of both the α and γ phosphorus nuclei. Based primarily on the temperature profile of the T_{1p}^{-1} data, it was assumed that this situation also holds true at higher temperatures.

Figures 8 and 9 are graphs of the averaged values of T_{2p}^{-1} and T_{1p}^{-1} obtained at different temperatures for all solutions. Values of the exchange rate, τ_M^{-1} , temperature dependence were obtained visually by drawing a tangent to the low temperature portions

of the curves, which are in the slow exchange region.

Figure 10 is a plot of $^{31}\text{P } \Delta\nu_{1/2\text{p}}$ vs $1/T$ for Gd(III) ITP. The concentration of gadolinium (III) in both solutions was the same, while that of ITP differed by a factor of ten. The ionic strength of both solutions was kept constant by adjusting the ionic strength of the weaker ITP solution, with tetramethyl ammonium nitrate. In comparison with the previous Figures, the data in Figure 10 were obtained only from a single run.

Possible hydrolysis of the nucleotide solutions was checked directly by the analysis of the phosphorus spectra, and hydrolysis was not observed. All curves to the data were drawn visually and all experimental data were found to be accurate to within $\pm 10\%$.

FIGURE 2: Proton decoupled natural abundance ^{13}C NMR spectra, measured at 311°K , for a 0.34M ATP solution. Metal ion concentrations due to the progressive addition of $\text{Gd}(\text{NO}_3)_3$ are indicated on each spectrum. The top spectrum is for a pure ATP solution.

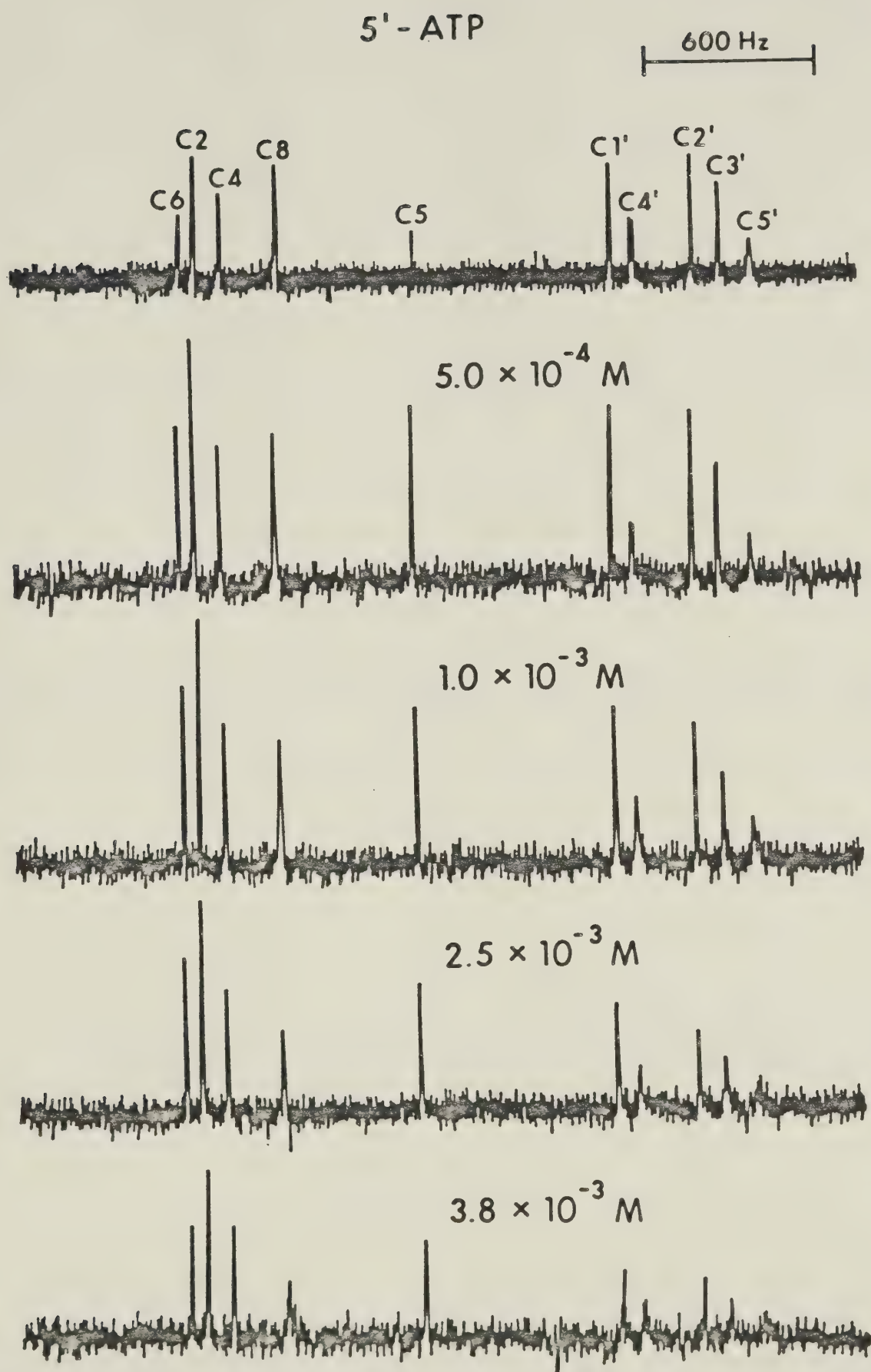


FIGURE 3: Proton decoupled natural abundance ^{13}C NMR spectra, measured at 308°K , for a 0.22M ITP solution. Metal ion concentrations of $\text{Gd}(\text{NO}_3)_3$ are indicated in a manner similar to that for Figure 2. The top spectrum is for a pure ITP solution.

5' - ITP

600 Hz

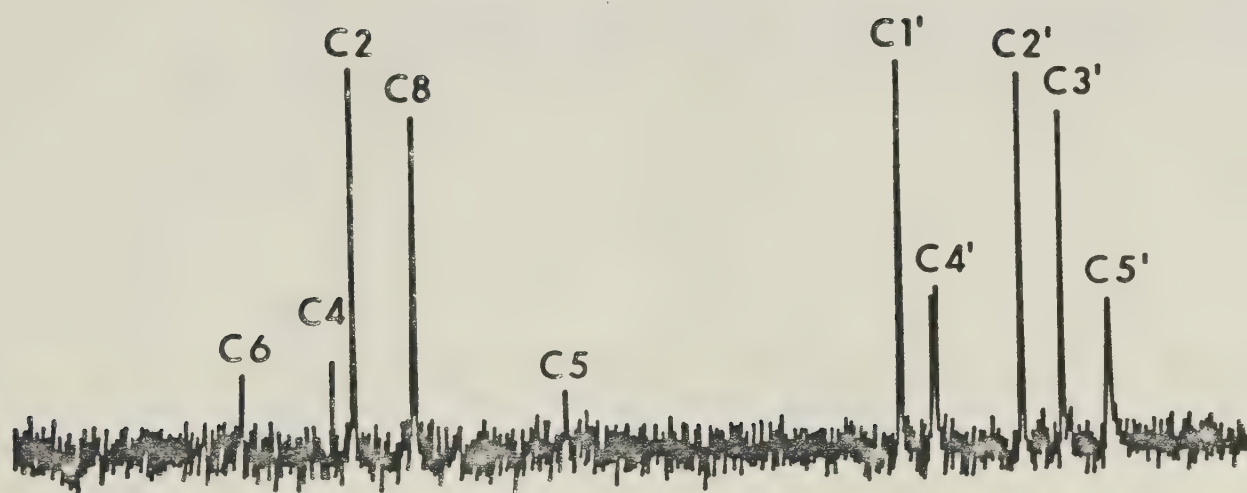
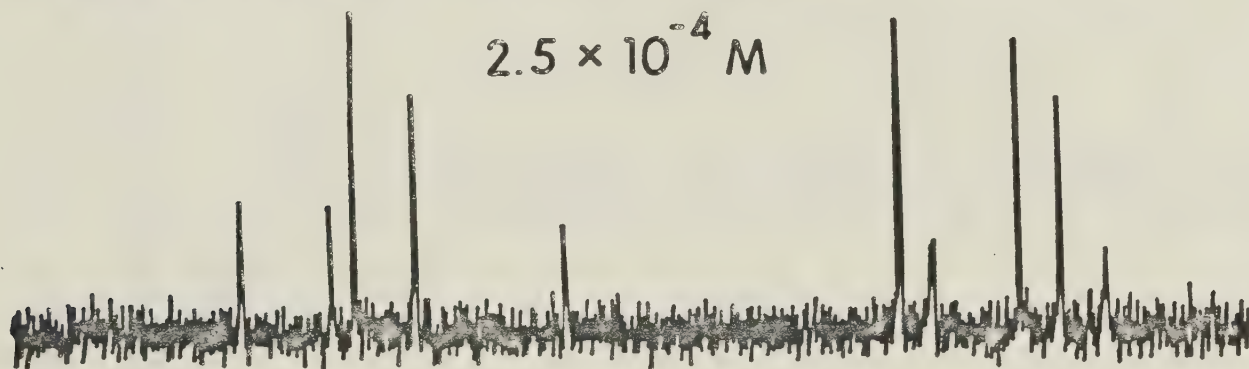
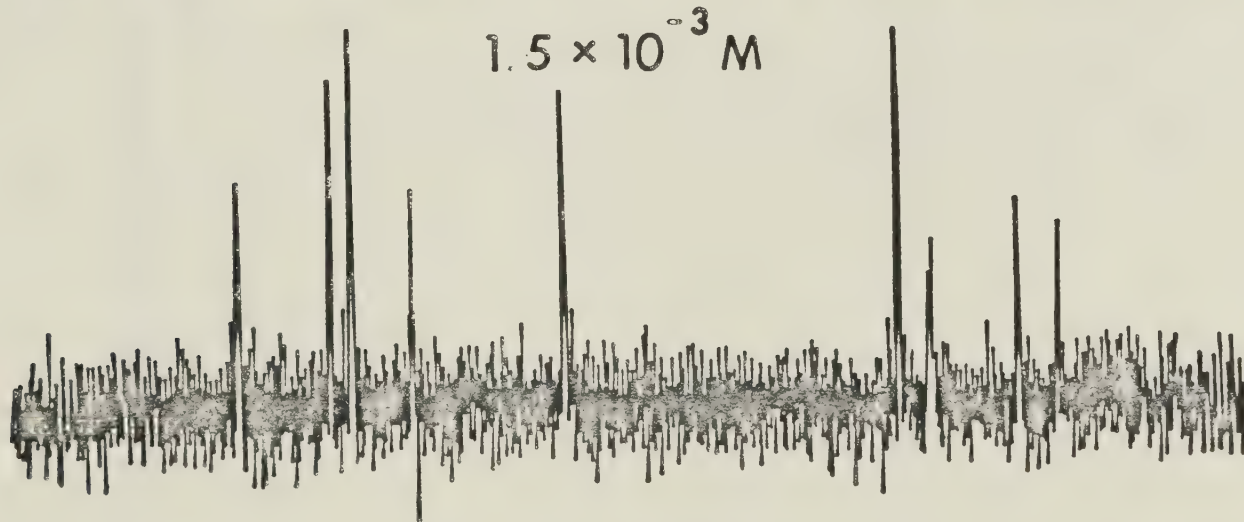
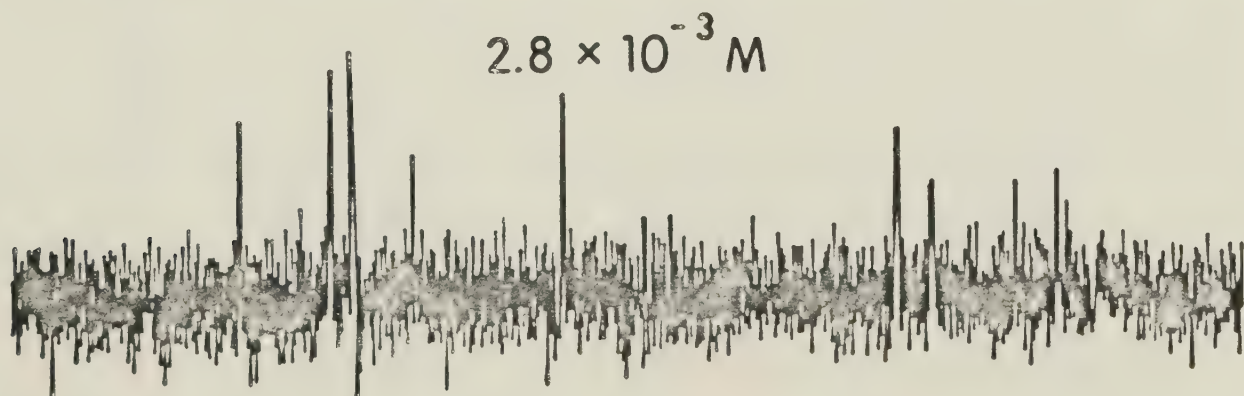
 $2.5 \times 10^{-4} \text{ M}$  $1.5 \times 10^{-3} \text{ M}$  $2.8 \times 10^{-3} \text{ M}$ 

TABLE I

 ^{31}P Paramagnetic Transverse Relaxation Time Measurements for Gd(III)-ATP Solutions

$f = [\text{Gd}]/[\text{ATP}]$	$\gamma = \text{Phosphorus}$			$\alpha = \text{Phosphorus}$		
	$10^3/T(^{\circ}\text{K}^{-1})$	$\frac{\Delta\nu}{2} \text{ (Hz)}$	$10^{-4}/f T_m \text{ (sec}^{-1}\text{)}$	$\frac{\Delta\nu}{2} \text{ (Hz)}$	$10^{-4}/f T_m \text{ (sec}^{-1}\text{)}$	
$2.5 \times 10^{-4}/0.33$	3.57	1.0	.42	1.1		.46
	3.45	2.0	.83	1.9		.79
	3.33	2.9	1.20	2.8		1.16
	3.26	5.8	2.41	5.7		2.37
	3.13	8.5	3.53	8.7		3.61
	3.23	9.4	3.90	9.2		3.82
	2.94	10.8	4.48	10.3		4.27
$4.3 \times 10^{-4}/.276$	3.51	-	-	2.7		.54
	3.39	4.5	.91	5.1		1.03
	3.28	8.3	1.67	8.6		1.73
	3.13	18.3	3.69	20.5		4.13
	2.98	21.7	4.37	23.9		4.81
	2.90	20.1	4.05	24.2		4.87
	2.82	17.7	3.56	22.6		4.55
$4.9 \times 10^{-4}/.276$	3.22	11.0	1.94	12.0		2.12
	3.12	22.5	3.97	22.7		4.01
$3.7 \times 10^{-4}/0.33$	3.57	0.7	.20	0.8		.22
	3.44	2.3	.64	2.3		.64
	3.27	5.0	1.40	5.0		1.40
	3.13	9.9	2.77	9.9		2.77
	3.03	12.4	3.49	12.6		3.53
	2.94	17.6	4.94	17.6		4.94
	2.86	17.7	4.96	17.7		4.96

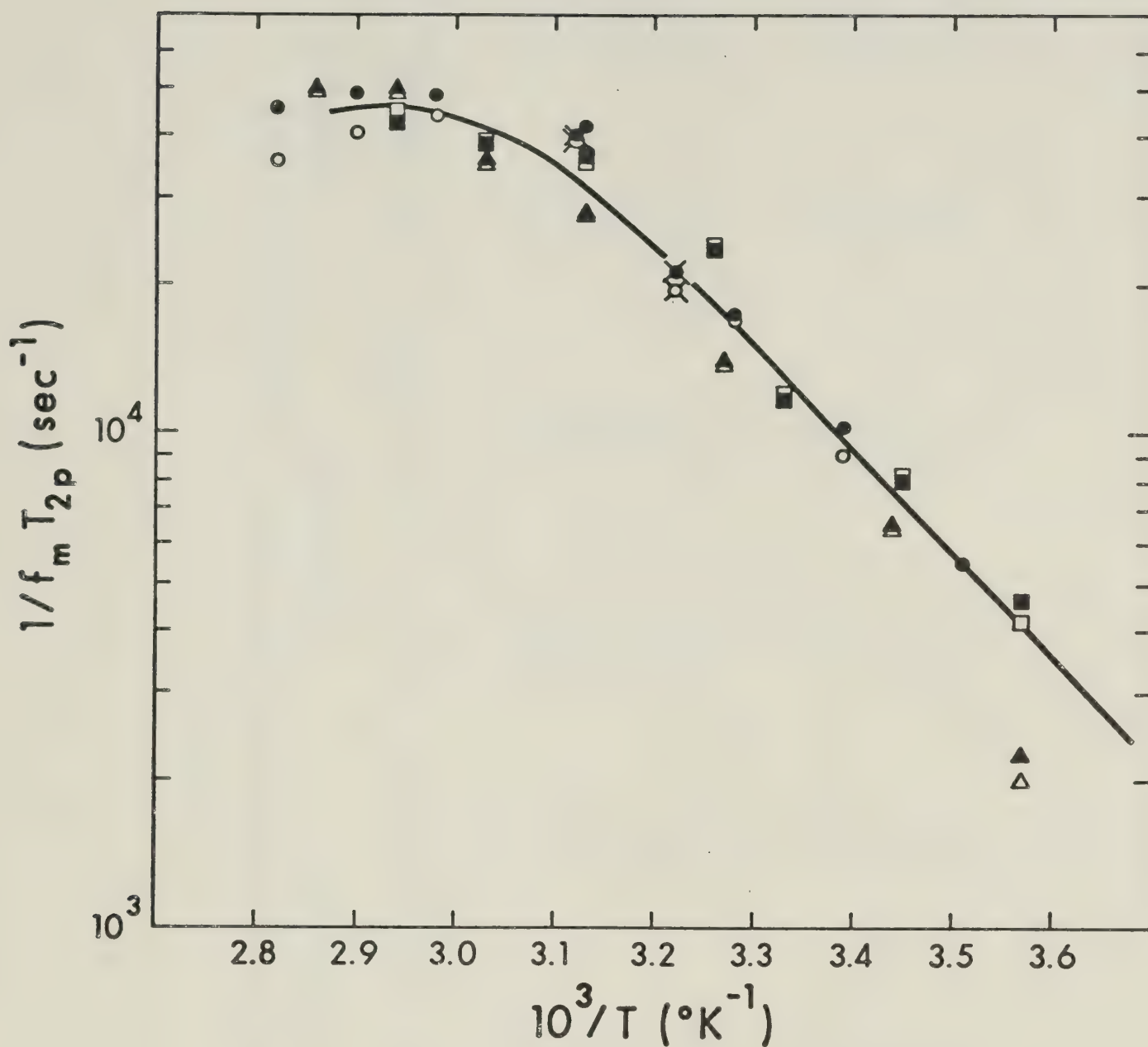


FIGURE 4: Temperature dependence of the ^{31}P paramagnetic transverse relaxation times for Gd(III)-ATP (see Table I).

LEGEND	Metal ion conc [M] x 10^4	2.5	4.3	4.9	3.7
		■	●	⊗	▲
		□	○	⊗	△

TABLE II

 ^{31}P Paramagnetic Longitudinal Relaxation Time Measurements for Gd(III)-ATP Solutions

$\frac{f}{m} = \frac{[\text{Gd}]}{[\text{ATP}]}$	$\frac{10^3}{T} (^{\circ}\text{K}^{-1})$	$\alpha = \text{Phosphorus}$		$\beta = \text{Phosphorus}$		$\gamma = \text{Phosphorus}$	
		T_{1p}^{-1}	$\frac{10^{-4}}{f} T_{1p}^{-1} (\text{sec}^{-1})$	T_{1p}^{-1}	$\frac{10^{-4}}{f} T_{1p}^{-1} (\text{sec}^{-1})$	T_{1p}^{-1}	$\frac{10^{-4}}{f} T_{1p}^{-1} (\text{sec}^{-1})$
$3.2 \times 10^{-4} / 0.276$	3.47	8.0	.65	6.9	.55	8.1	.65
	3.32	14.6	1.17	16.6	1.33	15.3	1.22
	3.25	20.9	1.68	22.7	1.82	21.1	1.67
	3.25	24.8	1.99	25.4	2.03	24.6	1.97
	3.15	31.6	2.53	34.4	2.76	32.3	2.59
	3.06	38.1	3.05	41.9	3.36	43.9	3.52
	2.96	48.4	3.88	52.2	4.18	47.4	3.80
	2.76	38.9	3.12	54.2	4.34	45.1	3.62
$1.0 \times 10^{-4} / 0.32$	3.56	1.3	.42	1.3	.42	1.1	.36
	3.44	2.3	.77	2.7	.88	2.5	.82
	3.27	5.2	1.73	6.1	2.00	6.1	2.00
	3.14	8.4	2.77	8.4	2.77	8.4	2.77
	2.99	10.5	3.47	11.0	3.63	10.4	3.43
	2.87	12.7	4.19	12.8	4.22	12.6	4.16

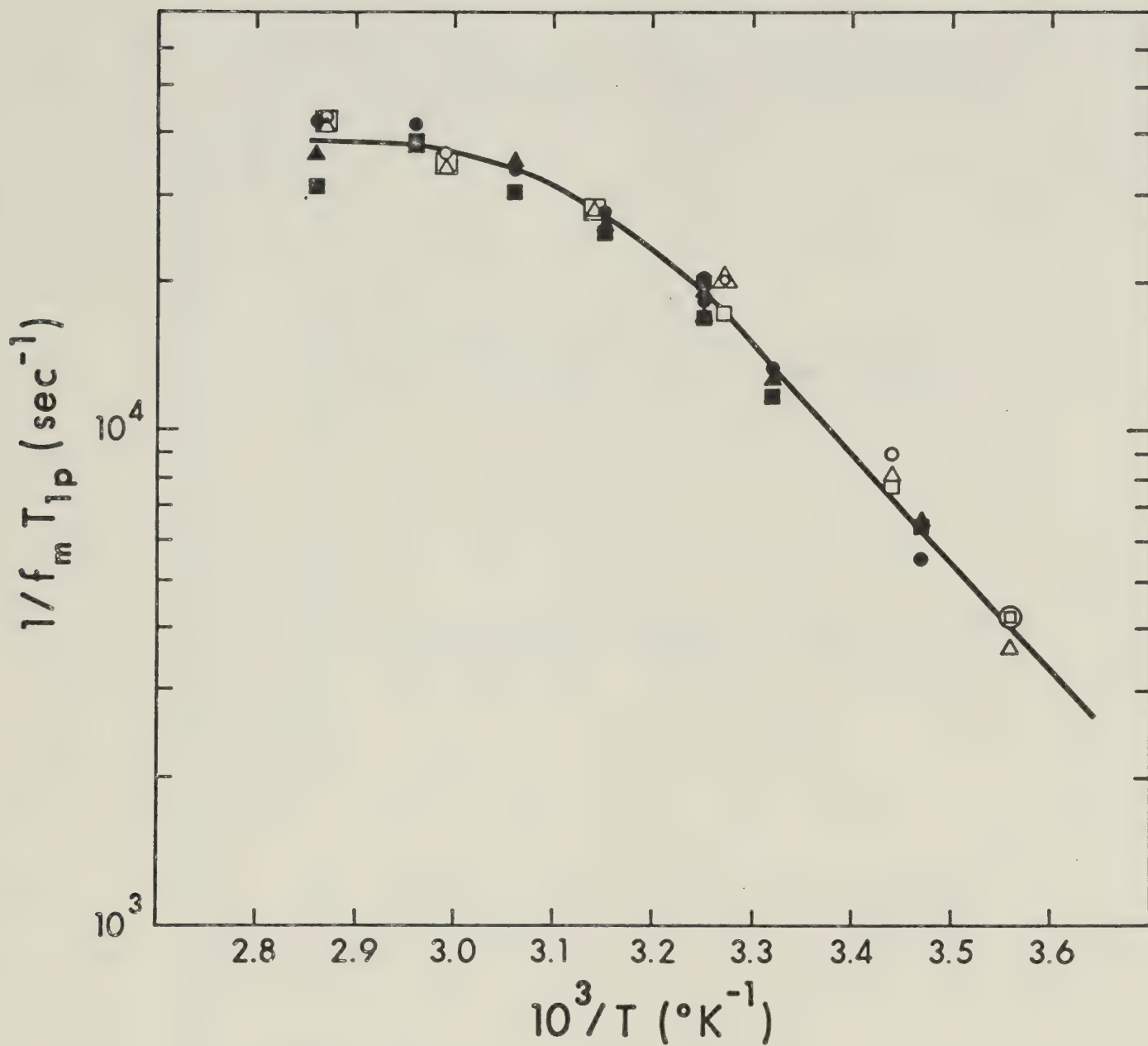


FIGURE 5: Temperature dependence of the ^{31}P paramagnetic longitudinal relaxation times for Gd(III)-ATP (see Table II).

LEGEND	Metal ion conc [M] $\times 10^4$		
		3.2	1.0
α		■	□
β		●	○
γ		▲	△

TABLE III

^{31}P Paramagnetic Transverse Relaxation Time Measurements for Gd(III)-ITP Solutions

$\frac{f}{m} = [\text{Gd}]/[\text{ITP}]$	$\frac{10^3}{T} (\text{K}^{-1})$	$\gamma = \frac{\text{Phosphorus}}{2}$		$\alpha = \frac{\text{Phosphorus}}{2}$	
		$\frac{\Delta\nu_{1\text{p}}}{2} (\text{Hz})$	$\frac{10^{-4}}{f T_m} (\text{sec}^{-1})$	$\frac{\Delta\nu_{1\text{p}}}{2} (\text{Hz})$	$\frac{10^{-4}}{f T_m} (\text{sec}^{-1})$
$2.5 \times 10^{-4} / .35$	3.39	1.7	.75	1.7	.75
	3.25	4.8	2.11	4.8	2.11
	3.16	6.5	2.86	6.4	2.81
	3.06	8.2	3.61	8.6	3.78
	2.98	11.0	4.84	11.0	4.84
	2.89	12.5	5.50	12.5	5.50
$5.0 \times 10^{-4} / .35$	2.81	14.0	6.16	14.0	6.16
	3.47	2.4	.53	2.6	.57
	3.37	4.7	1.03	4.2	.92
	3.30	7.2	1.58	7.7	1.69
	3.21	10.2	2.24	9.2	2.02
	3.57	2.0	.42	2.0	.42
$3.7 \times 10^{-4} / .25$	3.44	2.9	.60	2.8	.60
	3.27	6.1	1.28	6.1	1.28
	3.13	12.7	2.66	12.7	2.66
	3.03	15.0	3.14	15.0	3.14
	2.94	19.8	4.15	19.8	4.15
	2.86	21.0	4.40	20.0	4.19

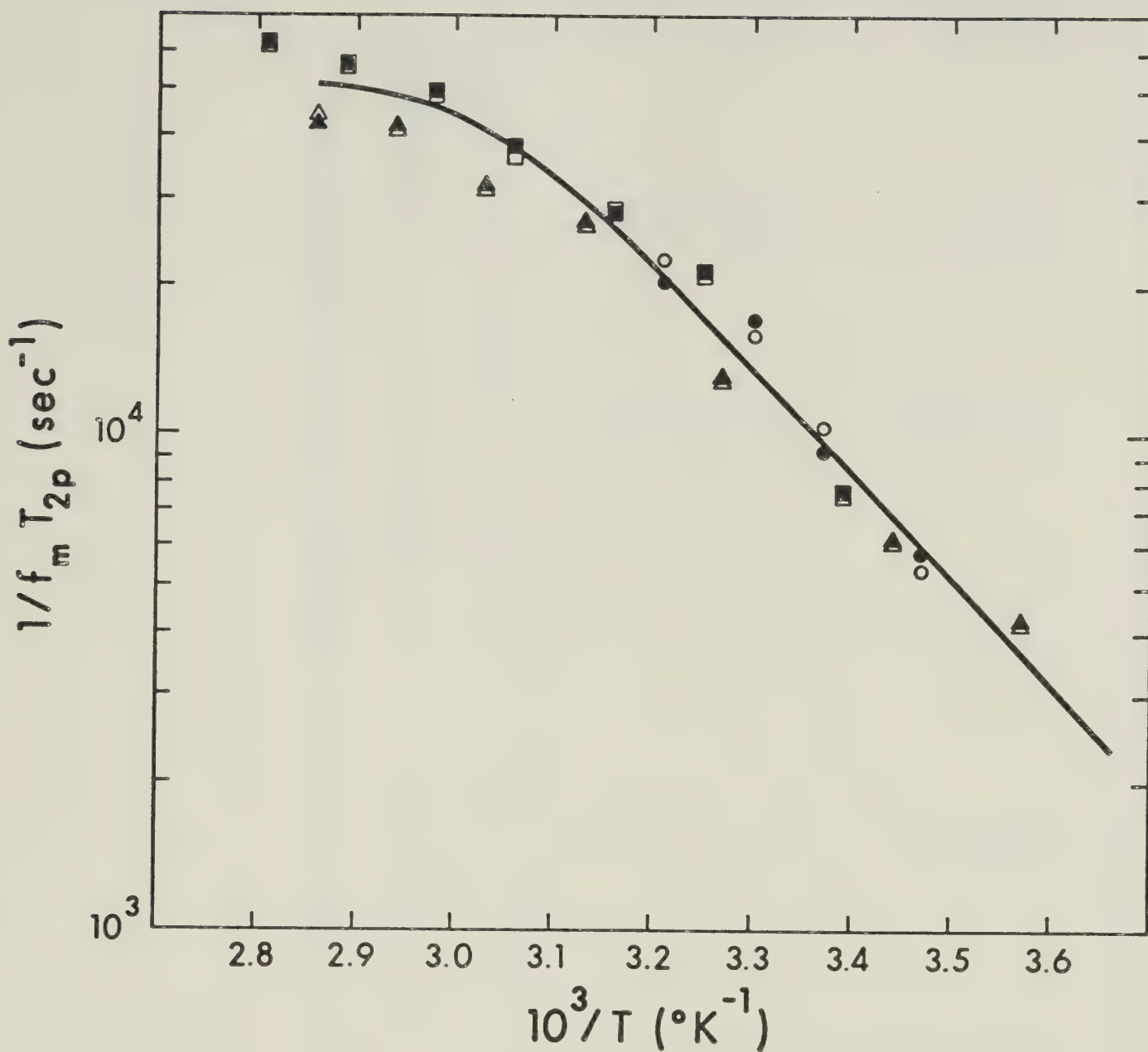


FIGURE 6: Temperature dependence of the ^{31}P paramagnetic transverse relaxation times for Gd(III)-ITP (see Table III).

LEGEND	Metal ion conc [M] x 10^4			
		2.5	5.0	3.7
α		■	●	▲
γ		□	○	△

TABLE IV

 ^{31}P Paramagnetic Longitudinal Relaxation Time Measurements for Gd(III)-ITP Solutions

$\frac{f}{m} = [\text{Gd}]/[\text{ITP}]$	$\frac{10^3}{T(^{\circ}\text{K}^{-1})}$	$T_1^{-1} \text{p}$	$\frac{10^{-4}}{f} \frac{T_1^{-1}}{m} (\text{sec}^{-1})$	$T_1^{-1} \text{p}$	$\frac{10^{-4}}{f} \frac{T_1^{-1}}{m} (\text{sec}^{-1})$	$T_1^{-1} \text{p}$	$\frac{10^{-4}}{f} \frac{T_1^{-1}}{m} (\text{sec}^{-1})$	$T_1^{-1} \text{p}$	$\frac{10^{-4}}{f} \frac{T_1^{-1}}{m} (\text{sec}^{-1})$	$T_1^{-1} \text{p}$	$\frac{10^{-4}}{f} \frac{T_1^{-1}}{m} (\text{sec}^{-1})$
$\alpha - \text{Phosphorus}$											
$\beta - \text{Phosphorus}$											
$\gamma - \text{Phosphorus}$											
$1.0 \times 10^{-4} / .35^*$	3.53	1.4	.50	1.6	.56	1.5	.53	1.5	.56	1.5	.53
	3.41	2.8	.98	3.0	1.05	2.9	1.01	2.9	1.05	2.9	1.01
	3.29	4.9	1.71	4.4	1.55	4.9	1.71	4.9	1.55	4.9	1.71
	3.26	5.8	2.01	5.8	2.01	5.8	2.01	5.8	2.01	5.8	2.01
	3.16	6.7	2.36	6.7	2.36	7.3	2.55	7.3	2.36	7.3	2.55
	3.11	8.0	2.81	7.7	2.69	8.0	2.81	8.0	2.69	8.0	2.81
	3.00	12.3	4.29	12.5	4.37	13.0	4.55	13.0	4.37	13.0	4.55
	2.90	12.5	4.37	12.5	4.37	12.5	4.37	12.5	4.37	12.5	4.37
$\alpha - \text{Phosphorus}$											
$\beta - \text{Phosphorus}$											
$\gamma - \text{Phosphorus}$											
$1.0 \times 10^{-4} / .35^*$	3.56	1.2	.44	1.3	.44	1.3	.44	1.3	.44	1.3	.44
	3.44	2.2	.78	1.9	.68	2.1	.74	2.1	.68	2.1	.74
	3.27	4.6	1.61	4.7	1.65	4.7	1.65	4.7	1.65	4.7	1.65
	3.13	8.3	2.90	8.1	2.82	8.3	2.90	8.3	2.82	8.3	2.90
	3.00	11.9	4.17	12.2	4.26	11.5	4.02	11.5	4.26	11.5	4.02
	2.87	11.8	4.13	11.2	3.92	11.8	4.13	11.8	3.92	11.8	4.13

* Two different solutions made up from the same [ITP] stock solution.

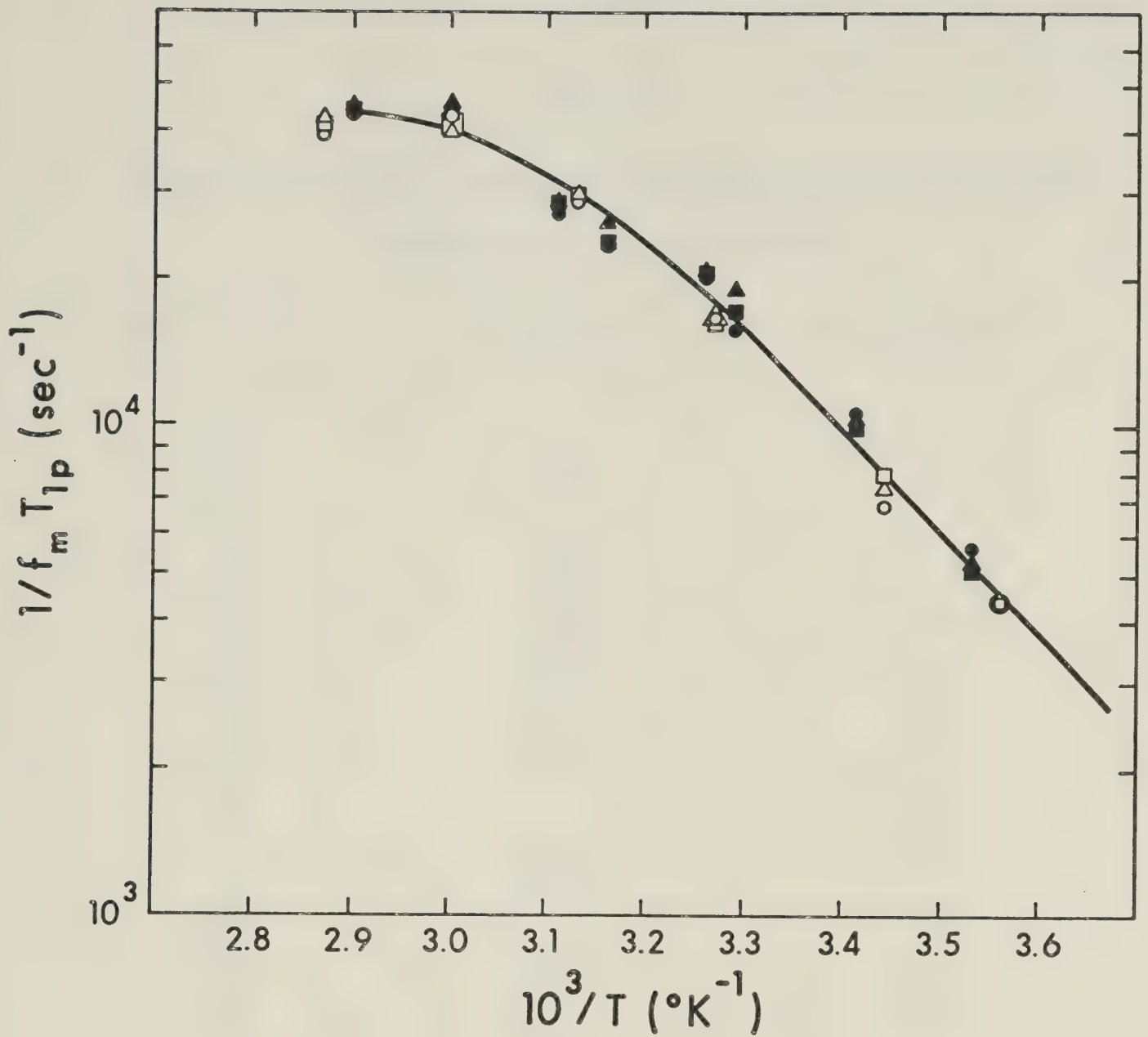


FIGURE 7: Temperature dependence of the ^{31}P paramagnetic longitudinal relaxation times for Gd(III)-ITP (see Table IV).

LEGEND	Metal ion conc [M] $\times 10^4$	1.0	
		■	□
	α	●	○
	β	▲	△
	γ		

TABLE V

Averaged Values of ^{31}P Paramagnetic Transverse and Longitudinal

Relaxation Times for Gd(III)-ATP

$10^3/T(^{\circ}\text{K}^{-1})$	$10^{-4}/\overline{f_m T_{2p}} (\text{sec}^{-1})$	$10^{-4}/\overline{f_m T_{1p}} (\text{sec}^{-1})$
3.57	.44	
3.56		.40
3.51	.54	
3.47		.62
3.45	.81	
3.44	.65	.82
3.39	.97	
3.33	1.18	1.24
3.28	1.70	
3.27	1.40	1.92
3.26	2.39	
3.25		1.87
3.22	2.05	
3.15		2.63
3.14		2.78
3.13	3.42	
3.12	3.99	
3.06		3.31
3.03	3.69	
2.98	4.62	3.51
2.96		3.96
2.94	4.38	
2.90	4.46	
2.87		4.19
2.86	4.97	3.69
2.82	4.08	

$\overline{T_{2p}}^{-1}$ = Average of values for α and γ for all solutions at that temperature.

$\overline{T_{1p}}^{-1}$ = Average of values for α , β and γ for all solutions at that temperature.

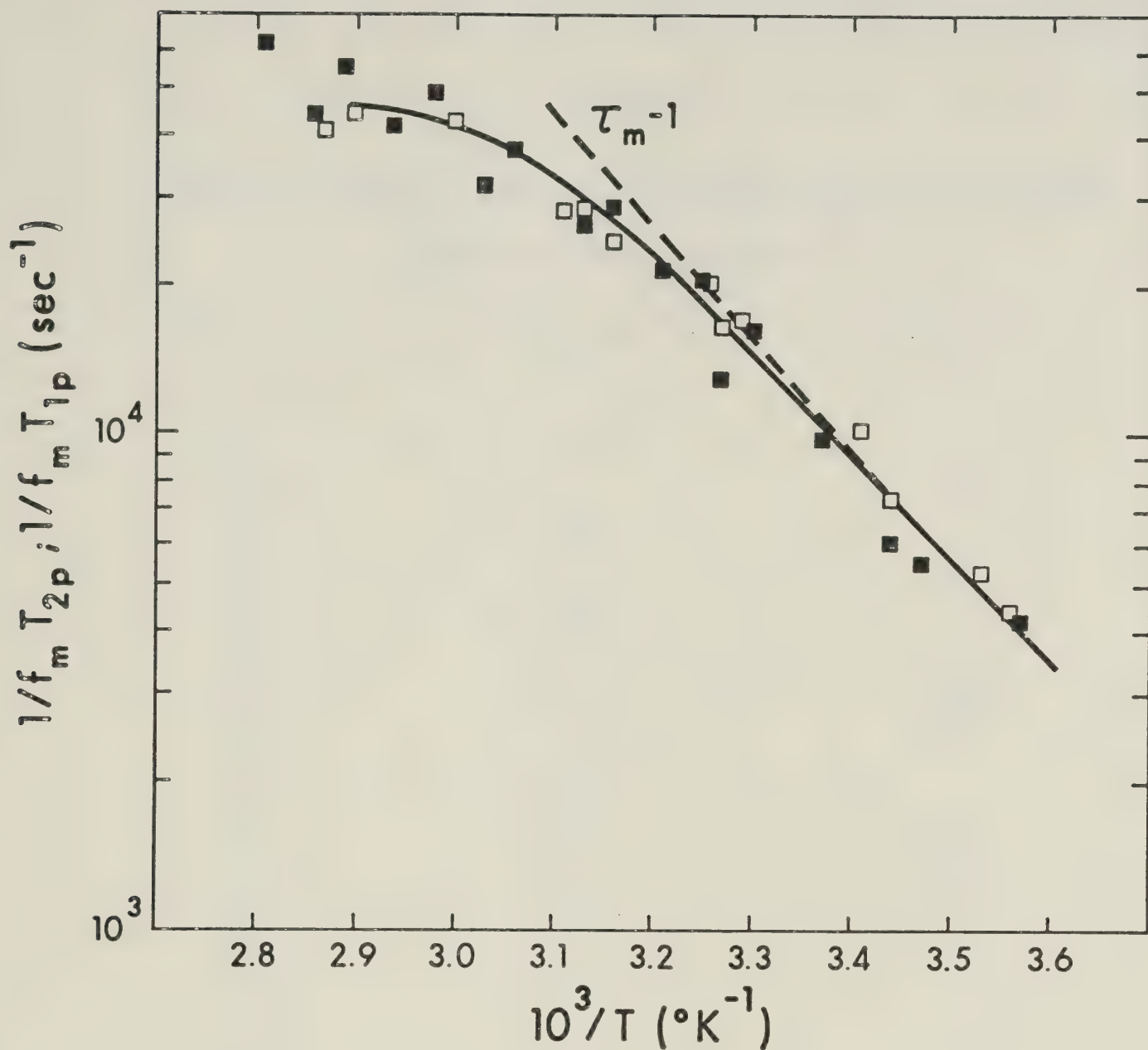


FIGURE 8: Temperature dependence of the averaged values of the ^{31}P paramagnetic transverse (■) and longitudinal (□) relaxation times for Gd(III)-ATP (see Table V).

TABLE VI

Averaged Values of ^{31}P Paramagnetic Transverse and Longitudinal

Relaxation Times for Gd(III)-ITP

$10^3/T(^{\circ}\text{K}^{-1})$	$10^{-4} \overline{f_m T_{2p}} (\text{sec}^{-1})$	$10^{-4} \overline{f_m T_{1p}} (\text{sec}^{-1})$
3.57	.42	
3.56		.44
3.53		.53
3.47	.55	
3.44	.60	.74
3.41		1.01
3.37	.98	
3.30	1.64	
3.29		1.71
3.27	1.28	1.63
3.26		2.01
3.25	2.11	
3.21	2.13	
3.16	2.85	2.42
3.13	2.66	2.18
3.11		2.78
3.06	3.70	
3.03	3.14	
3.00		4.28
2.98	4.84	
2.94	4.15	
2.90		4.38
2.89	5.50	
2.87		4.06
2.86	4.30	
2.81	6.16	

$\overline{T_{2p}}^{-1}$ = Average of values for α and γ for all solutions at that temperature.

$\overline{T_{1p}}^{-1}$ = Average of values for α , β and γ for all solutions at that temperature.

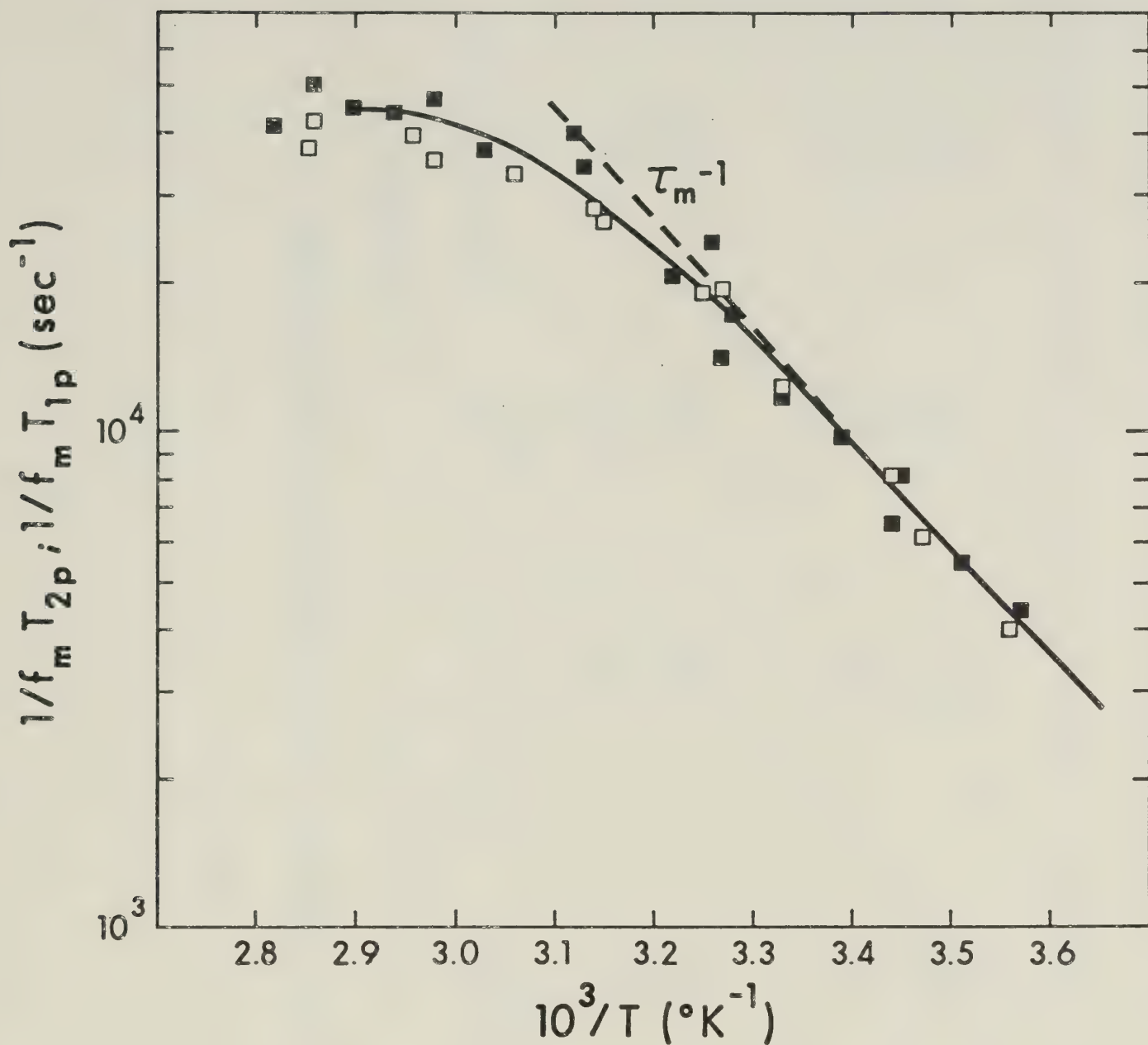


FIGURE 9: Temperature dependence of the averaged values of the ^{31}P paramagnetic transverse (■) and longitudinal (□) relaxation times for Gd(III)-ITP (see Table VI).

TABLE VII

 ^{31}P Paramagnetic Transverse Relaxation Time Measurements for Gd-ITP Solutions*

	$\gamma = \text{Phosphorus}$	$\alpha = \text{Phosphorus}$
$f = [\text{Gd}]/[\text{ITP}]$	$\frac{10^3/T(^{\circ}\text{K}^{-1})}{m}$	$\frac{10^{-4}/f T_m(\text{sec}^{-1})}{m}$
$1.25 \times 10^{-4}/0.010\text{M}$	$\frac{\Delta\nu_{1p}(\text{Hz})}{2}$	$\frac{\Delta\nu_{1p}(\text{Hz})}{2}$
	10.0	11.8
	17.0	18.5
	30.5	32.7
	34.5	36.5
41.0	47.0	
	.25	.30
	.43	.47
	.77	.82
	.87	.92
	1.03	1.18
$1.25 \times 10^{-4}/0.10\text{M}$	1.3	1.3
	2.3	2.3
	5.5	5.5
	10.0	10.0
	13.5	14.5
17.0	17.0	
	.33	.33
	.58	.58
	1.38	1.38
	2.51	2.51
	3.39	3.64
	4.27	4.27

* The ionic strength was maintained constant for both solutions by adding tetramethyl ammonium nitrate to the 0.01M ITP solution.

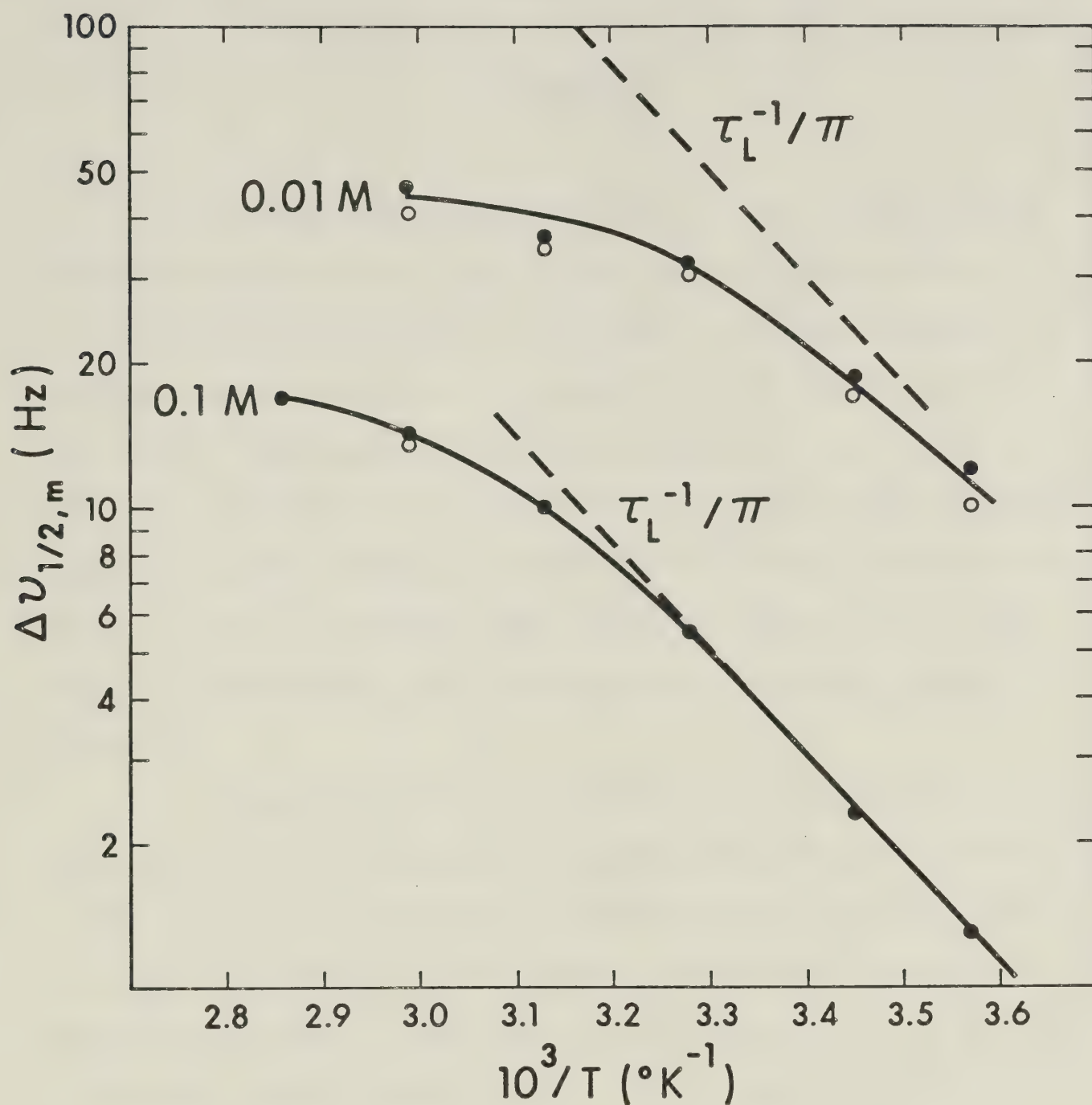


FIGURE 10: Temperature dependence of the ^{31}P paramagnetic linewidth measurements of the α (●) and γ (○) phosphates for Gd(III)-ITP solutions. Dotted lines indicating the slow exchange limit were drawn in visually by curve fitting the above data to those of Figure 9 (see Table VII).

CHAPTER FIVE

DISCUSSION

The reason for carrying out the ^{13}C NMR analysis was to determine whether or not a ring interaction was present between gadolinium (III) and the base. For ATP, the strong broadening of the ribose carbons followed by a weaker effect on the adenine C-8 was observed upon progressive metal ion additions. The observed effect on the ribose carbon nuclei indicates a strong metal ion binding with the phosphate oxygens (confirmed by the ^{31}P data). The magnitude of T_{2p} for the ^{31}P nuclei was about ten times greater, for the same metal ion concentration, than that observed at the ribose carbons or carbon C-8.

In order to determine any information concerning the conformation of the metal ion - nucleotide system from the induced broadening of the ^{13}C resonances, two restrictions must be met (49). The first of these is that the observed paramagnetic transverse relaxation time must be controlled by the relaxation rate of the bound nucleus and secondly, that this effect must be due primarily to dipolar interactions (i.e. controlled by fast exchange without significant contact terms). In relaxation measurements the absence of contact interactions for lanthanide ions has been previously documented (35). This situation also appears to be true for the Gd(III) - ITP and Gd(III) - ATP systems since the ^{31}P data in Figures 8 and 9 show that, within experimental error, T_{1M} and T_{2M} are equal. As far as the ^{13}C line broadening effects are concerned, these are not controlled by the

slow exchange mechanism. If this were the case, an equal broadening of all the carbon resonances of the adenine and/or the ribose portions of the nucleotide would be observed. Since this was not observed (Figures 2 and 3) the ^{13}C paramagnetic relaxation times are controlled by the fast exchange mechanism. The analysis of the spectra in Figure 2 indicates that there is no effective ring interaction between the metal ion and the nucleotide. This conclusion is in agreement with previous work (23-28). The broadening effects at C-5', C-4' and C-3' are a secondary effect resulting from the strong metal ion binding to the phosphorus oxygens. In addition, since the broadening effect at C-8 is not larger than that observed for the ribose carbon nuclei, it is also probably a weak "through space" interaction induced by the proximity of the phosphate bound metal ion to the H-8 proton. The ITP data of Figure 3 are in agreement with the ATP data to the extent that no ring interaction is indicated. The apparent discrepancy observed at the C-8 position is not a significant effect and has been observed before (50,51).

The data in Figures 4 to 9 indicate that, for the phosphorus nuclei, $T_{1p}^{-1} = T_{2p}^{-1}$ for the α , β and γ phosphates, for both nucleotides. In addition, T_{ip}^{-1} for ITP is equal to T_{ip}^{-1} for ATP ($i = 1$ or 2). This can be readily seen by comparing the projected τ_M^{-1} values in Figures 8 and 9, which are equal within experimental error. These τ_M^{-1} values are assumed to be in the "slow exchange" region.

According to the expression for T_{1p}^{-1} given in equation 15, outer sphere effects (T_{1os}^{-1}) may contribute to the longitudinal relaxation time. Since the expression for T_{1os}^{-1} (same as T_{2os}^{-1}

(eq: 14)) is similar to T_{1M}^{-1} (i.e. τ_c is the same form for both expressions) outer sphere control of T_{1p}^{-1} will show a frequency dependence. In addition, as mentioned in the theory section, a negative slope in the plot of T_{1p}^{-1} vs T^{-1} that is controlled by fast exchange will also show a frequency dependence.

In order to prove that the portion of the curve for T_{1p}^{-1} in Figures 8 and 9, with a negative slope is indeed in the slow exchange region (i.e. τ_M^{-1}) and that the turn-over region at higher temperatures is due to the effect of T_{1M}^{-1} , further variable frequency ^{31}P experiments were carried out. The basic procedure and instrumentation for this experiment was described in Chapter 3. The results indicate that the observed free induction decay measured at two different ^{31}P frequencies (23.98 MHz, 12.20 MHz) have the same null point (i.e. $\tau_0 = 50$ ms). Therefore,

$$\tau_0(\alpha, \beta, \gamma)_{23.98} = \tau_0(\alpha, \beta, \gamma)_{12.20} \quad [25]$$

and, accordingly to equation 23, it can be seen that (43)

$$\tau_0 = \text{constant}(T_{1p}) \quad [26]$$

Therefore

$$T_{1p}(23.98 \text{ MHz}) = T_{1p}(12.20 \text{ MHz}) \quad [27]$$

In conclusion, since a frequency dependence was not observed for T_{1p}^{-1} in the region where a "negative" activation energy term prevails, then the observed paramagnetic relaxation times for both Gd(III)-ITP and Gd(III)-ATP solutions are controlled at the lower temperatures exclusively by slow exchange. In this case, the fast exchange mechanism will control the high temperature portion since outer sphere effects are not expected to prevail in this region (34).

As a result, the conclusion is that the same exchange rate is observed for all three phosphorus nuclei and, in addition, the metal ion binds equally to the three phosphate oxygens. This second conclusion is based on the high temperature portion of the curves (Figures 8 and 9) where the progressive appearance of fast exchange does not impart any differences in the phosphorus T_{1p}^{-1} values as were observed for Mn-ATP (11). Since the three phosphorus nuclei have the same correlation time then, due to the r^{-6} dependence for both T_{1M}^{-1} and T_{2M}^{-1} , significant differences in the fast exchange relaxation time resulting from different metal - ligand distances would be observed. In addition, the bend-over region (i.e. region where T_{2p}^{-1} is controlled equally by T_{2M}^{-1} and τ_M^{-1}) would not be the same for all three nuclei. Since both the paramagnetic transverse and longitudinal relaxation times are equal within experimental error, over the temperature range under study (0°C to 60°C), the assumption that α , β and γ are equally bound to the metal ion appears quite valid.

A very recent paper by Tanswell et al (16), and to my knowledge, the only paper on this subject deals exclusively with the conformation of lanthanide ion complexes with ATP. Their experiments with Pr(III), Nd(III), Eu(III) and Yb(III) indicated that the ATP proton lanthanide shifts are entirely pseudocontact in nature. The experiments were performed under conditions where the metal ion and the nucleotide concentrations were nearly equal ($\sim 0.02\text{ M}$). Observed ^{31}P shifts were found to contain significant contact contributions which once corrected for resulted in equal pseudocontact shifts for the α and

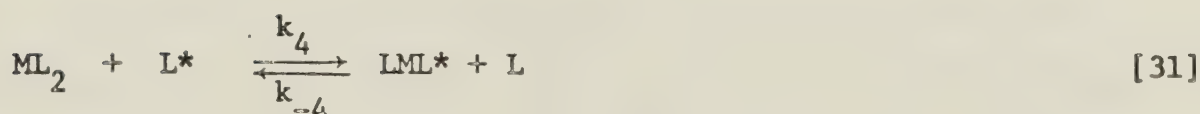
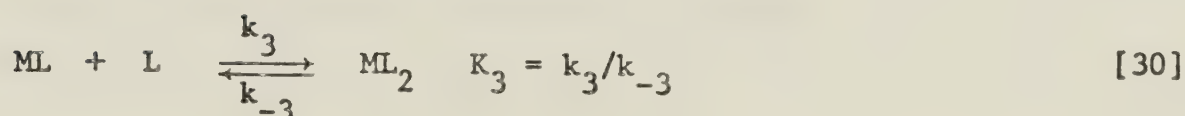
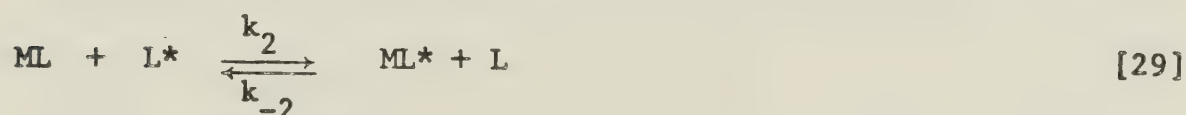
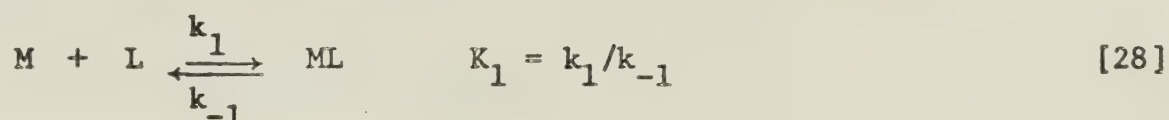
β phosphorus resonances. The smaller pseudocontact contribution observed for the γ phosphorus is presumably due to the fact that at a pH of 6.0 the terminal phosphate is still highly protonated (52). A computer analysis including both ^1H and ^{31}P data was performed and a satisfactory fit for the ^1H data could be obtained only if the lanthanide ions bind predominately to the β and γ phosphate oxygens and are further removed from the α phosphorus. This apparent reversal was considered acceptable due to the large error limits in the ^{31}P data. Their use of the lanthanide gadolinium (III) is limited since Gd(III) is primarily a broadening agent. However, their proton $T_{1\rho}$ data for the metal indicates that there is no effective ring interaction which is in agreement with the present ^{13}C results.

Kinetic Study of Gd(III) - ITP

In this discussion, two points concerning the kinetics need to be discussed. The first of these concerns the possibility of the Gd(ITP)_2 (ML_2) species; which must be considered in addition to the Gd(ITP) (ML) species since gadolinium (III) has a large co-ordination number (35,53) and the experimental conditions are such that $[\text{L}] \gg [\text{M}]$. Secondly, it has been shown (54) that for the Mn(II) (ATP) complex, two NMR exchange mechanisms are present in solution and that one of these show a kinetic dependence on the ligand concentration term $[\text{L}]$. The latter of these two points introduces an interesting problem, namely that of a 3 - site exchange rather than a 2 - site exchange which was developed in the theory section. Recent analyses of the three site case, (55,56) have shown

that for fast exchange, $T_{2p}^{-1} = \sum X_i T_{2i}^{-1}$ where T_{2i} is the transverse relaxation of the nucleus in site i and X_i is the corresponding concentration or rate constant ratio. For the slow exchange region, the expression for T_{2p}^{-1} becomes $T_{2p}^{-1} = \sum \tau_{ij}^{-1}$ where τ_{ij} is the lifetime of the nucleus in site i with respect to the $i \rightarrow j$ exchange. These results are of great importance since they indicate that the qualitative analysis of fast and slow exchange, developed so far in this thesis in terms of two site exchange, is just as valid for the three site case.

Having thus introduced the possibility of the ML_2 species as well as the concept of different exchange mechanisms, the kinetics for the Gd(III)-ITP system can be described in terms of a combination of 4 steps

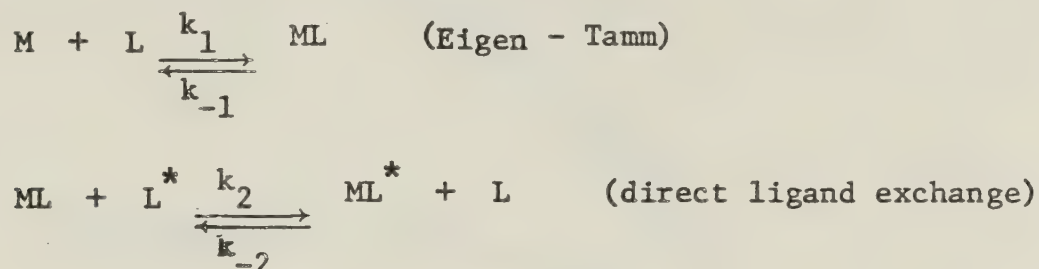


The unbound ligand term L , is formally dependent upon the degree of stacking. However, such stacking effects are due to intermolecular effects and are not expected to compete with the larger metal - nucleotide stability constants.

At this point, in order to simplify the analysis, two possibilities will be discussed.

CASE 1:

The ML_2 complex does not exist in solution and only the ML complex is present. In this case, equations 30 and 31 may be omitted and two mechanisms remain:



This particular system has been studied in detail by Pearson and Lanier (57) and Kuntz and al (54) and expressions for the slow exchange region have been derived as follows:

$$\tau_L^{-1} = k_1[M] + k_2[ML] \quad [32]$$

Since for mechanism (28) the following relationship is valid:

$$\tau_M/\tau_L = k_1[M]/k_{-1}$$

Then by substitution, equation 32 becomes:

$$\tau_M^{-1} = k_{-1} + k_2[L] \quad [33]$$

The lifetime τ_L , corresponds to species L as it exchanges from one environment to another. A plot of $\Delta\nu_{1/2p}$ vs T^{-1} is shown in Figure 10 for the ligand "L" as a function of the concentration of L. (A similar plot has been given for the Mn(II)-ATP system (54)). These data were then normalized and replotted in Figure 11 from which it can be seen that τ_M^{-1} does not show any dependence on [L] (within experimental

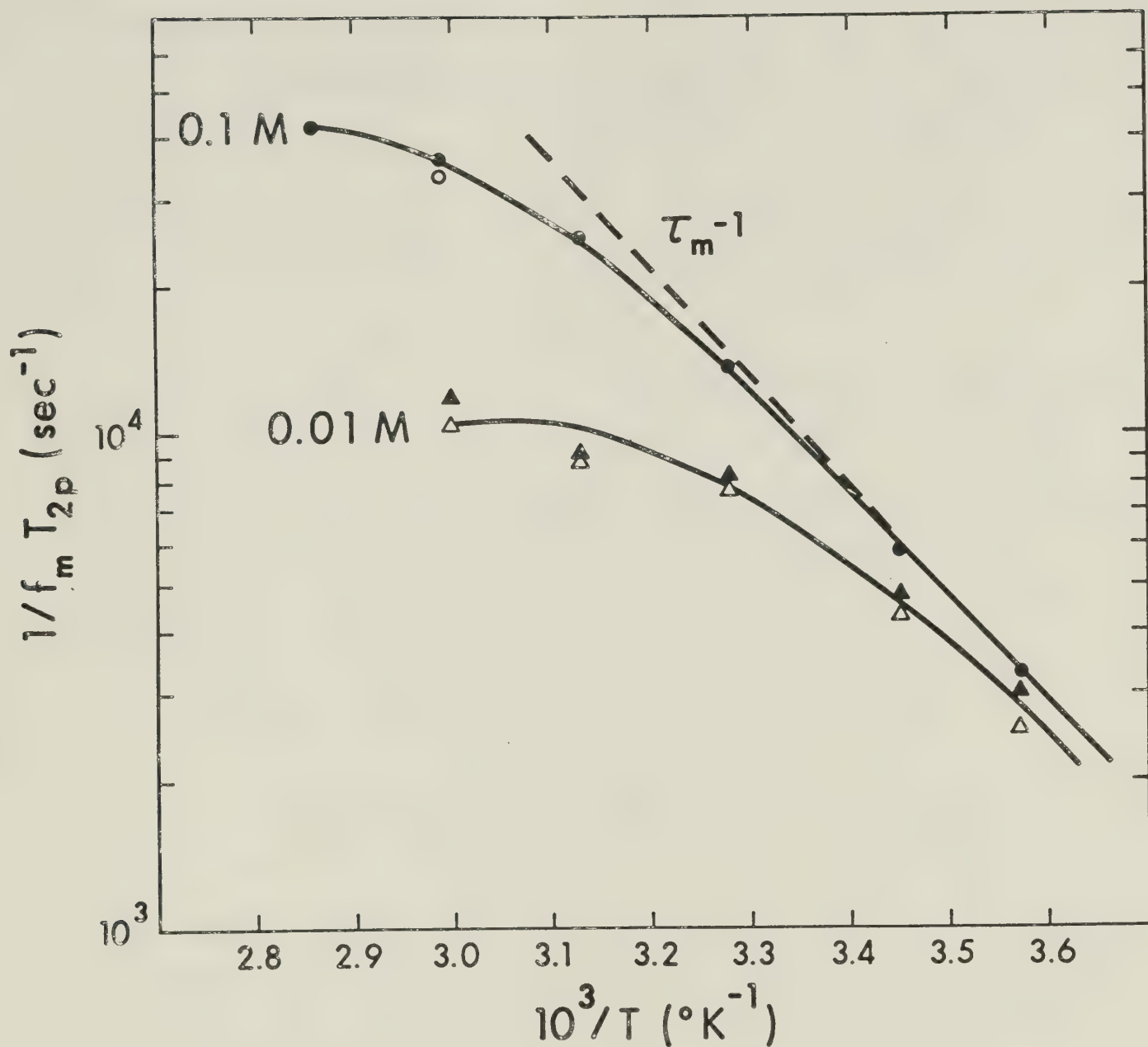


FIGURE 11: A plot of $(f_m T_{2p})^{-1}$ vs $1/T$ for Gd(III)-ITP solutions (see Figure 10 and Table VII).

LEGEND α (● ▲)
 γ (○ △)

error). Hence the direct ligand exchange mechanism does not contribute to any significant extent to τ_M^{-1} ; and equation 33 then simplifies to the form $\tau_M^{-1} = k_{-1}$.

From Figure 11 (as well as Figure 9) it can be seen that at 25°C, $\tau_M^{-1} = k_{-1} = 1.5 (+0.5) \times 10^4 \text{ sec}^{-1}$. In addition Valentine and Cottam (17) calculated a dissociation constant of 0.1 μM for Gd-ATP (pH=6.0, $\mu = 0.1\text{M}$, $T = 28^\circ\text{C}$). Since $K_1 = k_1/k_{-1}$ and putting in the proper numbers one obtains a value of $k_1 = 1.5(+1) \times 10^{11} \text{ sec}^{-1}$ at 25°C. The magnitude of this number must be considered suspect since a diffusion control limit in the range of 10^{10} sec^{-1} (58) would be expected for this system. This apparent discrepancy is quite significant since it indicates that the Gd(III)-ITP system should be analyzed in terms of an ML_2 species. In the above calculation it was assumed that the dissociation constant for the Gd-ATP system can be applied to the Gd-ITP system.

If we now turn our attention to equation 10 and use the appropriate values for the exchange rate τ_M^{-1} , then $\Delta H^\ddagger = 10.6 \text{ Kcal mole}^{-1}$ which compares quite well with that for Mn(II)-ATP (11) and Mn(II)-ITP (59) ($\Delta H^\ddagger = 11 \text{ Kcal mole}^{-1}$). However, the exchange rate τ_M^{-1} is about an order of magnitude longer than that observed for the Mn(II)-ITP system ($2.3 \times 10^5 \text{ sec}^{-1}$) (59). The exact reason for this is not known.

CASE 2:

The ML_2 complex does exist in solution. For this case, all four steps illustrated by equations 28 to 31 must be considered in order to obtain an expression for τ_L^{-1} .

Therefore

$$\begin{aligned}\tau_L^{-1} &= \frac{\partial [L]}{\partial t} \frac{1}{[L]} = k_1 \frac{[M][L]}{[L]} + k_2 \frac{[ML][L]}{[L]} + k_3 \frac{[ML][L]}{[L]} \\ &\quad + k_4 \frac{[ML_2][L]}{[L]} \\ \tau_L^{-1} &= k_1 [M] + k_2 [ML] + k_3 [ML] + k_4 [ML_2] \quad [34]\end{aligned}$$

In equation 34, the term $k_1 [M]$ may be neglected since a free metal ion concentration $[M] < 10^{-10} M$, (observed when $K_1 = 10^7$ and assuming $K_3 \geq 10^2$) implies that $k_1 \geq 10^{11} \text{sec}^{-1}$, which is greater than the diffusion control limit. Expressing the concentration of ML in terms of ML_2 and making several substitutions equation 34 now becomes

$$\tau_L^{-1} / [ML_2] = (k_2/K_3 + k_{-3}) (1/[L]) + k_4 \quad [35]$$

Any further analysis of the slow exchange region for Case 2 is limited by an assumption concerning the magnitude of the term K_3 . Specifically: if the stability constant (K_3) is large enough so that $[ML_2]$ does not change significantly with $[L]$, then the direct dependence of τ_L^{-1} on the concentration term $[L]$ indicated in Figure 10 implies that $(k_2/K_3 + k_{-3})$ contributes to the τ_L^{-1} while the term (k_4) does not.

In Figures 10 and 11, different turn over regions are observed for the 0.1M[ITP] and 0.01M[ITP] solutions, indicating that at the higher temperatures $T_{2p}^{-1}(0.01)$ and $T_{2p}^{-1}(0.1)$ are not equal.

According to equation 9 there are two factors (i.e. f_m , T_{2M}^{-1}) which control the observed transverse relaxation time while under fast exchange control. If we assume that the T_{2M}^{-1} (specifically τ_{cl}^{-1}) term is the same for both the 0.1M and 0.01M cases then whatever differences there may exist in T_{2p}^{-1} originate from the normalization term f_m . Since the concentration of the metal (M) is the same for both cases and the ligand (L) is in excess, then the bound sphere concentration (ML_2) can change only if the stability constant K_3 is small enough to permit a significant change in $[ML_2]$ with $[L]$ (54). If on the other hand K_3 is large (i.e. $[ML_2]$ constant) then the fact that the 0.01M Gd(III)-ITP enters the fast exchange region at a lower temperature than the 0.1M Gd(III)-ITP solution can be explained as a result of the reduction of the stacking of the ligand "L" in solution. This phenomenon would result in a smaller metal ion - ligand complex (i.e. decreased ligand stacking) in solution. Hence the rotational tumbling rate τ_R^{-1} of the complex would be faster; τ_{cl}^{-1} would be smaller and therefore T_{2p}^{-1} would be controlled by T_{2M}^{-1} at lower temperatures (equation 11).

Summary

The present results indicate that for the Gd(III)-ATP and Gd(III)-ITP systems, the metal ion binds equally to all three phosphate oxygens, that the extent of this binding is the same for both nucleotides, and that there is no significant metal ion ring interaction in either case. In addition, it appears that there is a significant difference in the interaction of the metal ions Gd(III) and

Mn(II) with the adenosine and inosine triphosphate systems. In fact, although this study is not conclusive in terms of the structure of the species in solution, it does appear to indicate that gadolinium (III) resembles the alkaline earths (16-20) more than manganese (II) in terms of binding to nucleotides.

Of great importance remains the question concerning the nature of the gadolinium (III) - nucleotide complex in solution. In order to show beyond any doubt that the ML_2 complex does exist, a more extensive kinetic analysis must be carried out to determine the magnitude of K_3 . This might be best achieved through the use of techniques such as laser T-jump where the individual rates of dissociation and association could be observed. To conclude, however, that the ML_2 species does not exist requires that we accept, based on this study, an unusually large rate constant for the $M + L \rightarrow ML$ association as well as a bound sphere relaxation extremely sensitive to nucleotide stacking.

REFERENCES

1. A. L. Lehninger, "Biochemistry", 2nd. ed., Worth Publishers Inc., 387 (1975).
2. R. M. Izatt, J. J. Christensen and H. J. Rytting, Chemical Reviews, 71, 439 (1971).
3. R. A. Dwek, "N.M.R. in Biochemistry", Oxford Press, 174 (1975).
4. "Metal Ions in Biological Systems", H. Sigel (ed.), Dekker Press, Vol. 1-4 (1974).
5. M. Cohn, Quart Reviews Biophys., 3, 61 (1970).
6. B. L. Vallee in "The Enzymes", Part B, Vol. 3, P. D. Boyer, H. Lardy and K. Myrbäc (ed.), Academic Press, New York (1960).
7. R. A. Dwek, R. J. P. Williams and A. V. Xavier, "Metal Ions in Biological Systems", H. Sigel (ed.), Dekker Press, 4, 64 (1974).
8. H. Sternlicht, R. G. Shulman and E. W. Anderson, J. Chem. Phys., 43, 3133 (1965).
9. Y. F. Lam, G. P. P. Kuntz and G. Kotowycz, J. Amer. Chem. Soc., 96, 1834 (1974).
10. M. Cohn and T. R. Hughes, J. Biol. Chem., 237, 176 (1962).
11. F. F. Brown, I. D. Campbell, R. Henson, C. W. J. Hirst and R. E. Richards, Eur. J. Biochem., 38, 54 (1973).
12. H. Sternlicht, R. G. Shulman and E. W. Anderson, J. Chem. Phys., 43, 3123 (1965).
13. H. Sternlicht, D. E. Jones and K. Kustin, J. Amer. Chem. Soc., 90, 7110 (1968).
14. V. Wee, I. Feldman, P. Rose and S. Gross, J. Amer. Chem. Soc., 96, 103 (1974).

15. M. S. Zetter, H. W. Dodgen and J. P. Hunt, *Biochemistry*, 12, 778 (1973).
16. J. Reuben, *Naturwissenschaften*, 62, 172 (1975).
17. K. M. Valentine and G. L. Cottam, *Archives of Biochemistry and Biophysics*, 158, 346 (1973).
18. R. A. Dwek, R. E. Richards, K. G. Moralle, E. Nioboën, R. J. P. Williams and A. V. Xavier, *Eur. J. Biochem.*, 21, 204 (1971).
19. A. Levitzki and J. Reuben, *Biochemistry*, 12, 204 (1971).
20. H. Hauser, M. C. Phillips, B. A. Levine and R. J. P. Williams, *Eur. J. Biochem.*, 58, 133 (1975).
21. J. Reuben, *J. Phys. Chem.*, 75, 3164 (1971).
22. J. Reuben, *Biochemistry*, 10, 2834 (1971).
23. P. Tanswell, J. M. Thornton, A. J. Korda and R. J. P. Williams, *Eur. J. Biochem.*, 57, 135 (1975).
24. C. D. Barry, A. C. North, J. A. Glasel, R. J. P. Williams and A. V. Xavier, *Nature*, 232, 236 (1971).
25. C. D. Barry, D. R. Martin, R. J. P. Williams and A. V. Xavier, *J. Mol. Biol.*, 84, 491 (1974).
26. C. M. Dobson, R. J. P. Williams and A. V. Xavier, *J. Chem. Soc. (Dalton)*, 1762 (1974).
27. C. D. Barry, C. M. Dobson, R. J. P. Williams and A. V. Xavier, *J. Chem. Soc. (Dalton)*, 1765 (1974).
28. C. D. Barry, J. A. Glassel, R. J. P. Williams and A. V. Xavier, *Biochem. Biophys. Acta*, 262, 101 (1972).
29. O. Kennard, N. W. Isaacs, W. D. S. Molherwell, J. C. Coppola, D. L. Wampler, A. C. Larson and D. G. Watson, *Proc. Roy. Soc. London Sec. A. Math. Phys. Sci.*, 325, 401 (1971).

30. M. S. Mohan and G. A. Rechnitz, J. Amer. Chem. Soc., 94, 1714 (1972).
31. H. M. McConnell, J. Chem. Phys., 28, 430 (1958).
32. F. Block, Phys. Rev., 70, 460 (1946).
33. T. J. Swift and R. E. Connick, J. Chem. Phys., 37, 307 (1962).
34. T. J. Swift in "NMR of Paramagnetic Molecules Principles and Applications", G. N. La Mar, W. De W. Horrocks Jr. and R. H. Holm (eds.), New York, New York, Academic Press (1973).
35. R. A. Dwek, "N.M.R. in Biochemistry", Oxford Press, 192 (1973).
36. I. Solomon, Phys. Rev., 99, 559 (1955).
37. N. Bloembergen, J. Chem. Phys. 27, 572 (1957).
38. R. E. Connick and D. Fiat, J. Chem. Phys., 44, 4103 (1966).
39. Z. Luz and S. Meiboom, J. Chem. Phys., 40, 2686 (1964).
40. M. Rubinstein, A. Baram and Z. Luz, Mol. Phys., 20, 67 (1971).
41. N. Bloembergen and L. O. Morgan, J. Chem. Phys., 34, 842 (1961).
42. A. Hudson and J. Lewis, Trans. Faraday Soc., 66, 1297 (1970).
43. A. I. Vogel, "A Textbook of Quantitative Inorganic Analysis", 3rd. ed., 433 (1961).
44. T. C. Farrar and E. D. Becker, "Pulse and Fourier Transform N.M.R." Academic Press, 20 (1971).
45. R. Freeman and H. D. W. Hill, J. Chem. Phys., 51, 3140 (1969).
46. D. E. Dorman and J. D. Roberts, Proc. Nat. Acad. Sci. U. S. A., 65, 19 (1970).
47. A. J. Jones, M. W. Wimbley, D. M. Grant and R. K. Robins, Proc. Nat. Acad. Sci. U. S. A., 65, 27 (1970).
48. H. H. Mantsch and I. C. P. Smith, Biochem. Biophys. Res. Comm., 46, 430 (1972).

49. W. G. Espersen and R. B. Martin, J. Phys. Chem., 80, 161 (1976).
50. G. V. Fazakerley, J. C. Russell and M. E. Wolfe, J. Chem. Soc. Chem. Comm. 527 (1975).
51. H. Sigel, C. F. Naumann and B. Prys, Eur. J. Biochem., 41, 209 (1974).
52. R. M. Smith and R. A. Alberty, J. Phys. Chem., 60, 184 (1956).
53. R. Jones, R. A. Dwek and S. Forsen, Eur. J. Biochem., 47, 271 (1974).
54. G. P. P. Kuntz, Y. F. Lam and G. Kotowycz, Can. J. Chem., 53, 926 (1975).
55. H. W. Dodgen, A. D. Jordan and R. B. Jordan, J. Phys. Chem., 77, 2149 (1973).
56. N. S. Angerman and R. B. Jordan, Inorg. Chem., 8, 1824 (1969).
57. R. G. Pearson and R. D. Lanier, J. Amer. Chem. Soc., 86, 765 (1964).
58. E. F. Caldin, "Fast Reactions in Solutions", Wiley Press, (1964).
59. G. P. P. Kuntz and G. Kotowycz, Biochemistry, 14, 4144 (1975).

B30171